

**DUAL-WAVELENGTH PASSIVE Q-SWITCHED FIBER LASER BY
USING $(\text{Ti}_3\text{Al}(\text{Co}_0.5, \text{Ni}_0.5)_2)$ D-SHAPED FIBER AS A SATURABLE
ABSORBER**

RONALD RAJ A/L ROBERT

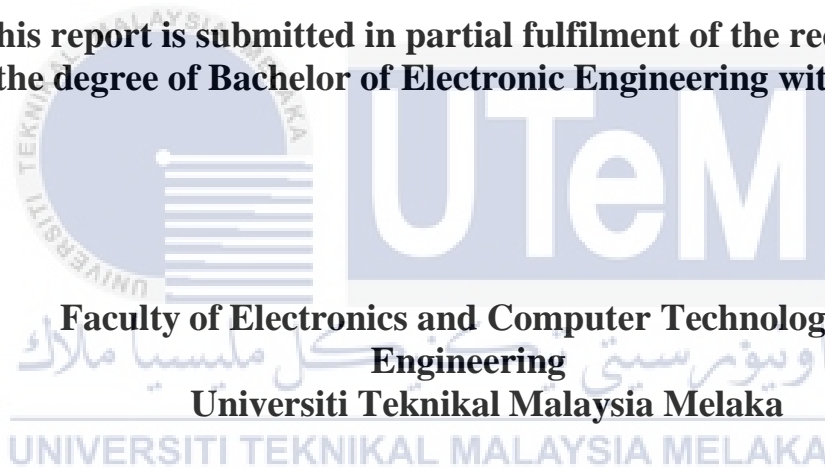


UNIVERSITI TEKNIKAL MALAYSIA MELAKA

**DUAL-WAVELENGTH PASSIVE Q-SWITCHED FIBER LASER BY USING
(Ti₃Al (Co_{0.5}, No_{0.5})₂) D-SHAPED FIBER AS A SATURABLE ABSORBER**

RONALD RAJ A/L ROBERT

**This report is submitted in partial fulfilment of the requirements
for the degree of Bachelor of Electronic Engineering with Honours**



2024

**BORANG PENGESAHAN STATUS LAPORAN
PROJEK SARJANA MUDA II**

Tajuk Projek : Dual-wavelength Passive Q-switched Fiber Laser by using $(\text{Ti}_3\text{Al}(\text{Co}_5, \text{No}_5)_2$ D-Shaped Fiber as a Saturable Absorber

Sesi Pengajian : 2023/2024

Saya RONALD RAJ A/L ROBERT mengaku membenarkan laporan Projek Sarjana Muda ini disimpan di Perpustakaan dengan syarat-syarat kegunaan seperti berikut:

1. Laporan adalah hakmilik Universiti Teknikal Malaysia Melaka.
2. Perpustakaan dibenarkan membuat salinan untuk tujuan pengajian sahaja.
3. Perpustakaan dibenarkan membuat salinan laporan ini sebagai bahan pertukaran antara institusi pengajian tinggi.
4. Sila tandakan (✓):

SULIT*

(Mengandungi maklumat yang berdarjah keselamatan atau kepentingan Malaysia seperti yang termaktub di dalam AKTA RAHSIA RASMI 1972)

TERHAD*

(Mengandungi maklumat terhad yang telah ditentukan oleh organisasi/badan di mana penyelidikan dijalankan.)

TIDAK TERHAD



(TANDATANGAN PENULIS)

Disahkan oleh:



(COP DAN TANDATANGAN PENYELIA)

Alamat Tetap: No 28, Jalan Akasia 6, Taman Akasia, 75150, Bukit Baru, Melaka.

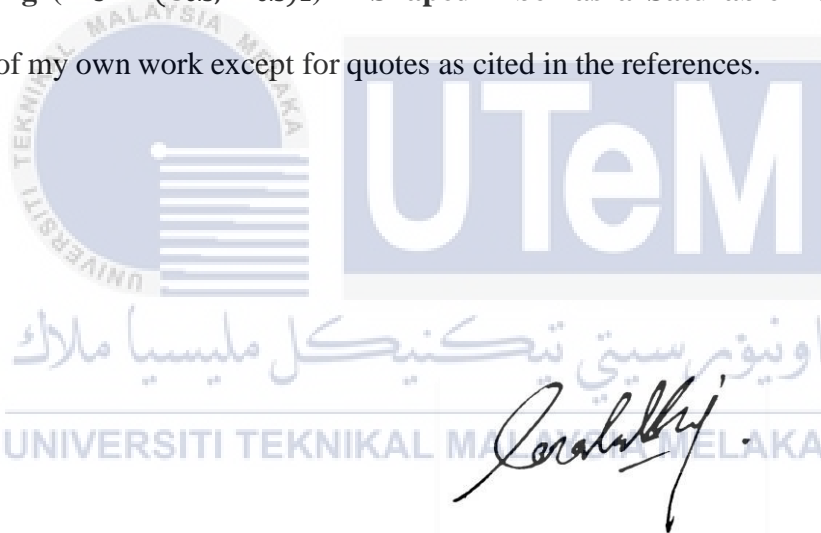
Tarikh : 15 Januari 2024

IR. DR. ANAS BIN ABDUL LATIFF
Pensyarah Kanan
Fakulti Teknologi Dan Kejuruteraan Elektronik Dan Komputer (FTKEK)
Universiti Teknikal Malaysia Melaka (UTeM)

Tarikh : 24 Januari 2024

DECLARATION

I declare that this report entitled “**Dual-wavelength Passive Q-switched Fiber Laser by using $(\text{Ti}_3\text{Al}(\text{Co}_0.5, \text{No}_0.5)_2$ D-Shaped Fiber as a Saturable Absorber**” is the result of my own work except for quotes as cited in the references.



Signature :

Author : RONALD RAJ A/L ROBERT
.....

Date : 15 JANUARY 2024
.....

APPROVAL

I hereby declare that I have read this thesis and in my opinion this thesis is sufficient in terms of scope and quality for the award of Bachelor of Electronic Engineering with Honours.



اونيور سيكنيكل مليسيا ملاك
Anas

Signature :

UNIVERSITI TEKNIKAL MALAYSIA MELAKA

IR. DR. ANAS BIN ABDUL LATIFF

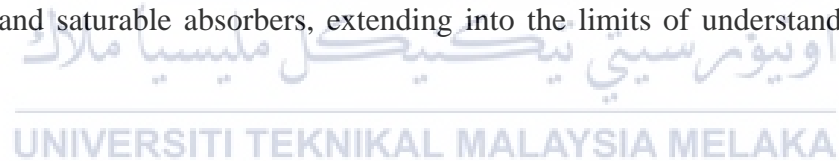
Pensyarah Kanan

Supervisor Name : **Fakulti Teknologi Dan Kejuruteraan Elektronik Dan Komputer (FTKEK)**
Universiti Teknikal Malaysia Melaka (UTeM)

Date : 24 JANUARY 2024
.....

DEDICATION

This thesis is dedicated to my beloved photonics members, supervisor, parents, family members and friends for their endless support and encouragement. Furthermore, this thesis pays tribute to the innovators in the fields of fiber optics, laser technology, and materials science who prepared the path for the execution of this research. It highlights the tireless efforts of researchers who explored into the complexities of D-shaped fiber optics and saturable absorbers, extending into the limits of understanding.



ABSTRACT

A saturable absorber (SA) called Titanium Aluminum Carbonitride, ($Ti_3Al(C_{0.5}, N_{0.5})_2$) D-shape fiber structure based on MAX-Phase material has been successfully developed. This SA is used to reliably generate a dual-wavelength Q-switched laser within the C-band region. Their optical properties are investigated and then incorporated within a cavity of an erbium-doped fiber laser to initiate a Q-switched operation. Comparison of the Q-switched laser parameters demonstrated a significant enhancement when using MAX-DS as the saturable absorber. The D-shaped, ($Ti_3Al(C_{0.5}, N_{0.5})_2$) structure is linked to two fiber ferules of a patch cord and incorporated into an erbium-doped fiber laser (EDFL) ring cavity. The Q-switched laser operates at two specific wavelengths, $\lambda_1=1532.36$ nm and $\lambda_2=1558.36$ nm. It remains stable within a pump power range of 38.06-75.5 mW. The MAX-DS Q-switched EDFL laser has achieved an enhanced repetition rate of 51.92 kHz and a significantly reduced pulse width of 3.57 μ s. The maximum peak power is calculated as 23.74 mW, while the pulse energy reaches a maximum of 84.74 nJ. The optical-to-optical efficiency is 7.81%, the maximum output power is 4.4 mW, and the signal-to-noise ratio is 60 dB. This demonstration indicates that the, ($Ti_3Al(C_{0.5}, N_{0.5})_2$) D-shape structure has the potential to serve as an alternative SA with excellent prospects in optical-related applications.

ABSTRAK

Penyerap tepu MAX-Phase (SA) yang dikenali sebagai Titanium Aluminium Carbonitride, ($Ti_3Al(C_{0.5}, N_{0.5})_2$) struktur D-shape berjaya dibangunkan untuk menunjukkan laser suis-Q yang boleh dipercayai dalam Rantau C-band untuk menjana dwi-panjang gelombang. Sifat optiknya disiasat dan menggabungkannya dalam rongga laser gentian dop erbium untuk memulakan suis-Q. Parameter laser Q-switched dibandingkan dan mendedahkan peningkatan yang ketara dengan menggunakan MAX-DS sebagai SA. Bentuk D ($Ti_3Al(C_{0.5}, N_{0.5})_2$) disambungkan kepada dua ferula gentian kord tampal dan disepadukan ke dalam rongga cincin laser gentian doped erbium (EDFL). Laser Q-switched, yang berpusat pada $\lambda_1=1532.36$ nm dan $\lambda_2=1558.36$ nm, muncul secara stabil pada julat kuasa pam 38.06-75.5mW. Laser EDFL Q-switched MAX-DS mempunyai kadar pengulangan tertinggi sebanyak 51.92 kHz dan lebar nadi paling sempit sebanyak 3.57 μ s. Kuasa puncak terkira maksimum ialah 23.74 mW, manakala tenaga nadi tertinggi ialah 84.74 nJ. Kecekapan optik-ke-optik sebanyak 7.81%, kuasa keluaran maksimum 4.4 mW dan nisbah isyarat-ke-bunyi sebanyak 60 dB. Demonstrasi ini mencadangkan bahawa ($Ti_3Al(C_{0.5}, N_{0.5})_2$) struktur bentuk D boleh menjadi SA alternatif yang mungkin mempunyai prospek yang baik dalam aplikasi berkaitan optik.

ACKNOWLEDGEMENTS

I would like to express my sincere appreciation to several individuals and organizations who have provided invaluable support throughout my academic journey. Firstly, I want to extend my heartfelt gratitude and thanks to my supervisor, Ir. Dr. Anas Bin Abdul Latiff (SV) and to my Co- supervisor Dr. Haziezol Helmi bin Mohd Yusof (Co-SV). Their enthusiasm, patience, and valuable suggestions, as well as his insightful comments, practical advice, and constant flow of ideas, have been instrumental in helping me with my research and the writing of this thesis. It was really a big help because I were having difficulty getting the project in beginning but due to their patience and tolerance, I managed to conduct the project.

I am extremely grateful to the Faculty of Electronics & Computer Technology and Engineering (FTKEK) for giving me the opportunity to pursue a degree in Electronic Engineering. I would also like to thank the lecturers of FTKEK for their guidance, suggestions, and feedback during my project at the university. Additionally, I would like to express my appreciation to my trainer, Muhammad Aizat Zaim Bin Zaini (Postgraduate Student) who guide, contribute his time and knowledges to me along completion of my project while express my appreciation to all the Photonics Laboratory staff and technicians who have provided their cooperation and made indirect or direct contributions to the completion of my project. A sincere acknowledgement in extended to our colleagues and collaborators which are Janzen and YiHen, whose varied expertise benefited this project, fostering

a collaborative environment of shared knowledge. Furthermore, I do believe that there is a lack and unintended mistake. Thus, with these opportunities I would like to seek apology for any insolence during development of this project.

I would like to express my sincere appreciation to my family for their unwavering support and encouragement throughout my degree study. Their constant presence has been a source of strength for me. Additionally, I am grateful to my friends for their friendship, moral support, and valuable advice, as they have played an essential role in my academic journey. Completing this project would not have been possible without their support.

To conclude, I extend my heartfelt gratitude to my supervisor, the Faculty of Electronics & Computer Technology and Engineering, my family, and my friends for their significant contributions and unwavering support during my degree study. Their assistance and encouragement have been invaluable, and I am truly grateful for their presence throughout my academic journey. I also hope that this project will be helpful towards the present and future generation to have an idea to innovate more useful technology in our society and for the good of the modernization world.

TABLE OF CONTENTS

Declaration	
Approval	
Dedication	
Abstract	i
Abstrak	ii
Acknowledgements	iii
Table of Contents	v
List of Figures	viii
List of Tables	ix
List of Symbols and Abbreviations	x
List of Appendices	xii
CHAPTER 1 INTRODUCTION	1
1.1. Project Introduction	2
1.2. Problem Statement	4
1.3. Research Objectives	6
1.4. Scope of Research	6
1.5. Hypothesis	7
1.6. Report Structure	8
CHAPTER 2 RESEARCH BACKGROUND	10

	vi
2.1 Overview of Fiber Laser	11
2.2 Fiber Pulsed Laser	12
2.3 Passive Technique	13
2.4 Ring Cavity	14
2.5 Erbium Doped Fiber Laser (EDFL)	15
2.6 Q-Switched Pulse Laser	16
2.7 Passive Q-Switched Pulse Laser	16
2.8 Saturable Absorber (SA)	18
2.9 Real Saturable Absorber	19
2.10 2D-Material	20
2.11 MAX-Phase as $(\text{Ti}_3\text{Al}(\text{Co}_0.5, \text{No}_0.5)_2)$	23
2.12 Integration of SA	24
2.13 D-Shape Fiber Optic	25
CHAPTER 3 METHODOLOGY	27
3.1 Brief Description of Methodology	27
3.2 Methods and technique used for experimental work	28
3.2.1 Fabrication of D-shape Fiber Optic	29
3.2.2 Preparation of MAX-Phase $(\text{Ti}_3\text{Al}(\text{Co}_0.5, \text{No}_0.5)_2)$	31
3.2.3 Configuration for Ring Cavity of Passive Q-Switched	34
CHAPTER 4 RESULTS AND DISCUSSION	37
4.1 Q-switched Laser Performance	39

4.2 Comparisons of previous research	vii 47
CHAPTER 5 CONCLUSION AND FUTURE WORKS	49
5.1 Conclusion	50
5.2 Future works	51
REFERENCES	54
LIST OF PUBLICATIONS AND PAPERS PRESENTED	61
APPENDICES	62



LIST OF FIGURES

Figure 2.0: K-chart of the research	62
Figure 2.1a: Ring Cavity	13
Figure 2.1b: Linear cavity	13
Figure 2.2: Artificial and real saturable absorbers	18
Figure 2.3: Classification of low-dimensional materials SA	19
Figure 2.4: The 2D materials SA	20
Figure 2.5: Integration Methods of SA	24
Figure 2.5a: Thin film-based SA	24
Figure 2.5b: Optical deposition technique	24
Figure 2.5c: D-shaped fiber metal-based material deposition	24
Figure 2.5d: Tapered optical fiber	24
Figure 3.0: Flow chart of methodology	28
Figure 3.1a: D-shape fiber preparation setup	29
Figure 3.1b: Graphical demonstration for mechanical D-shape fiber fabrication	29
Figure 3.1c: Microscopic image of the D-shape fiber	29
Figure 3.2a: $\text{Ti}_3\text{Al} (\text{C}_{0.5}, \text{N}_{0.5})_2$ MAX-Phase solution	31
Figure 3.2b: Preparation of PVA Solution	31
Figure 3.2c: Fabrication of $\text{Ti}_3\text{Al} (\text{C}_{0.5}, \text{N}_{0.5})_2$ MAX-Phase	31
Figure 3.3: MAX-Phase solution for integration	34
Figure 3.4: The schematic arrangement of MAX-Phase D-shape fiber in EDFL	34
Figure 4.0: The repetition rate and pulse width	39
Figure 4.1: The output power, pulse energy, and peak power	40
Figure 4.2: The output spectrum of the QS laser and CW laser	42
Figure 4.3a: The two-envelope pulse train	44

Figure 4.3b: Oscilloscope trace	ix 44
Figure 4.4a: The RF spectrum of the pulsed laser with span of 900kHz	46
Figure 4.4b: Fundamental frequency spectrum	46

LIST OF TABLES

Table 1.0: Tabulation of raw data of the experimental work	38
Table 2.0: Comparison of Laser output performance of Q-switched	47

LIST OF SYMBOLS AND ABBREVIATIONS

CW	:	Continuous wave
FL	:	Fiber laser
FBG	:	Fiber Bragg Grating
YDFL	:	Ytterbium Doped Fiber Laser
EDFL	:	Erbium Doped Fiber Laser
TDFL	:	Thulium Doped Fiber Laser
S-band	:	Short band
C-band	:	Conventional band
L-band	:	Long band
QS	:	Q-switched
ML	:	Mode-locked
SESAM	:	Semiconductor saturable absorber mirror
NOLM	:	Nonlinear optical loop mirror
NALM	:	Nonlinear amplifying loop mirror
SA	:	Saturable absorber
0D	:	Zero-dimensional
1D	:	One-dimensional
2D	:	Two-dimensional
QDs	:	Quantum dots
MAX-DS	:	MAX-Phase D-shape
GO	:	Graphene oxide
BP	:	Black phosphorus
TI	:	Topological insulator
TMD	:	Transition metal dihalide

REO	:	Rare-earth oxide
TF	:	Thin film
OD	:	Optical deposition
DSF	:	D-shape fiber
OSA	:	Optical spectrum analyzer
OPM	:	Optical power meter
OSC	:	Oscilloscope
FF	:	Fundamental frequency
RFSA	:	Radio frequency spectrum analyzer
SNR	:	Signal-noise ratio
RR	:	Repetition rate
PW	:	Pulse width
PP	:	Pulse period/Pump power/Peak power
PE	:	Pulse energy
OP	:	Output power
Ti ₃ Al C ₂	:	Titanium aluminum carbide
(Ti ₃ Al (C _{0.5} , N _{0.5}) ₂)	:	Titanium aluminum carbonitride
WDM	:	Wavelength division multiplexer
PDI	:	Polarization dependent isolator
PVA	:	Polyvinyl alcohol
LPE	:	Liquid-phase exfoliation
DI	:	Deionized
PD	:	Photodetector
InGaAs	:	Indium gallium arsenide
S-M-S	:	Single- multi- single mode fiber
D S-M-S	:	D-shape single- multi- single mode fiber
MZI	:	Mach Zehnder Interferometer

LIST OF APPENDICES

Figure 1.0: K-chart of the research

62



CHAPTER 1

INTRODUCTION



This chapter covers the introduction of the project. Furthermore, it highlights the problem of the current situation in the photonics industry that leads to the idea of development of the project. Moreover, this chapter will include the topics on project introduction, problem statement, research objectives, scope of research, hypothesis, and report structure.

1.1 Project Introduction

The development of a dual-wavelength passive Q-switched fiber pulsed laser has received significant interest in recent optical research due to the demand for versatile and efficient laser sources in various fields. This study investigates a holistic method to attain fiber laser technology involving a setup for a dual-wavelength passive Q-switched fiber pulse laser technique with use of single-notch D-shaped fiber optics, and incorporation of a MAX-Phase (2D-material) as a saturable absorber.

The passive technique relies on the inherent properties of the laser cavity components to manipulate the pulse characteristics, eliminating the need for external modulators. This allows for the creation of a dual-wavelength output with mode mismatched of D-shape structure. The incorporation of passive technique and D-shape enhances the simplicity and stability of the system.

Moreover, the presence of Q-switched operation amplifies the adaptability of the fiber laser system. Q-switched allows for the generation of pulses with high peak power by manipulating the quality factor (Q) of the laser cavity. The Q-switching technique temporally suppresses the laser emission until a high energy state is reached, followed by rapid release, resulting in intense pulses. This methodology was integrated into this study to enhance the potential for generating dual-wavelength pulses with maximized output performance.

Moreover, the research study into the D-shaped fiber optic exploring single notch configurations, with its unique structure, plays a crucial role in this integrated

system. The D-shaped fiber facilitates efficient mode coupling and wavelength division within a single fiber core, ensuring the simultaneous generation of dual wavelength. Its configuration allows for effective power transfer and mode conversion, contributing to the stability and reliability of the dual-wavelength pulse generation.

The key element that plays a crucial role in enabling the passive Q-switching operation is the saturable absorber made of MAX-Phase material. By utilizing the unique characteristics of 2D materials, MAX-Phase functions as an effective regulator for manipulating laser pulses. The laser's saturable absorption properties allow it to function in a Q-switched mode, producing short pulses with high peak powers. The combination of a single-notch D-shaped fiber optic and MAX-Phase material as a saturable absorber shows potential for enhance performances of the pulsed laser output.

To summarize, the combination of passive Q-switched technique and single-notch D-shaped fiber optic configurations has shown great potential for advancing dual-wavelength fiber pulsed laser technology.

1.2 Problem Statement

In recent years, the field of laser technology has experienced significant progress, leading to major developments that have wide-ranging implementation in various domains. However, the generation of a dual-wavelength passive Q-switched fiber pulsed laser occurred due to the presence of mode mismatched within the D-shaped fiber.

Current methodologies frequently depend on complex setups, which restrict their practicality for various applications. Continuous wave (CW) lasers are characterized by a constant power output, providing a continuous stream of energy. Besides, fiber pulsed lasers can achieve very high peak power levels during the short pulse duration, even if their average power is lower than that of CW lasers [1]. One issue arises from the limitations placed on active techniques. Although these techniques are successful in improved laser pulses, they frequently introduce complications in the preparation procedures, making them intricate and requiring significant resources. The complexity arises due to the need to integrate additional components, such as external modulators, in order to achieve the desired modulation. The complicated design of the system not only increases the expenses but also creates possible areas of failure, limiting the system's ability to scale and its reliability. Moreover, the dependence on active techniques contributes to the existing issue of a limited operating range in fiber lasers.

The versatility of fiber lasers for different applications is limited by their essential restriction to specific wavelengths. However, a fiber laser, which has a linear cavity configuration and meters of fiber length, is unable to generate a laser

output with a single frequency due to spatial hole burning in the gain medium. A common solution to this problem involves the use of a ring cavity. SESAMs are subject to various physical limitations, such as their considerable dimensions, inflexibility, restricted frequency range, low thresholds to damage, inability to serve as input/output couplers, intricate manufacturing process [11,12], high expense, become narrower operational bandwidth [13], and requirement for accurate spatial placement. These limitations make them impractical for deployment in fiber laser systems. In order to achieve passive Q-switched, the laser structure often incorporates saturable absorbers (SAs) in the form of unpumped sections within the laser cavity.

Artificial (SAs) are large in size and susceptible to environmental factors such as fiber displacement, temperature fluctuations, and vibrations, resulting in reduced efficiency of reproduction. The critical issues among 2D-materials research, including complex in the fabrication process, lower threshold power, a small absorption bandwidth, microstructure and composites. SA structure on previous research generate lot of losses, system unstable. 2D- material has discover such as graphene but MAX-Phase have not discovered yet because of new material. This is the reason that applying MAX-Phase D-shape as Saturable Absorber (SA). Thin Film and Optical deposition have limitation such as low damage threshold when adding up the pump power (mW) until limits the threshold. This is causing the film melt. Generation of dual-wavelength ankle due to light presence of more mismatched.

1.3 Research objectives

The primary goal of this research study is to generate dual-wavelength of continuous wave Fiber Laser with aided of MAX-Phase D-shaped Fiber Optic. The study aims to achieve the following specific objectives:

1. To develop dual-wavelength continues wave fiber laser based on D-shaped fiber and S-M-S configuration. [RO1]
2. To validate the MAX-Phase D-shaped fiber saturable absorber by generating Q-switching laser operation. [RO2]

1.4 Scope of research

Recognizing these challenges, this research is prompted by the imperative to address these limitations along exploring the potential of dual-wavelength fiber pulsed laser generation using a combination of passive Q-switching technique, D-shaped fiber optic, and MAX-Phase (2D material) as saturable absorber (SA). The Erbium-doped fiber lasers (EDFL) utilize a configuration that operates at a wavelength of 1.5 μm . This configuration offers a broader bandwidth, increased gain, and reduced attenuation in comparison to alternative laser systems. Material SA of $(\text{Ti}_3\text{Al}(\text{C}_{0.5}, \text{N}_{0.5})_2)$ MAX-Phase was used for this research. This is because MAX-Phase possesses unique physical properties, such as exceptional resistance to oxidation, a high modulus of elasticity, low density, and a high melting temperature, when compared to other 2D materials. This innovative approach aims to overcome the complexities associated with active technique, offering a more streamlined and

efficient solution. Moreover, the integration of passive technique and the unique attributes of D-shaped fiber optics present an opportunity to extend the operating wavelengths beyond the confines of thin film and optical deposition. In essence, this research seeks to carve a path toward a more versatile and accessible fiber laser technology, with implications spanning various industries and applications.

1.5 Hypothesis

There are three major hypotheses that can be listed out for this research study:

1. Design a D-shape fiber laser setup capable to generate dual wavelength in C-band region mode.
2. Investigate and implement passive Q-switched fiber laser technique to manipulate pulse characteristics without the need for external modulators, thereby improving the system's ease and stability.
3. Analyse the time-related properties of the generated pulses, such as pulse duration, repetition rate, and pulse energy, in order to figure out the changing actions of the system.

1.6 Report structure

This thesis is organized and structured into 5 significant chapters. Chapter 1 begins by providing an overview of the project, which includes defining the problem statement, research objectives, the scope of the research study and the hypothesis. Furthermore, the second chapter of this project focuses a theoretical evaluation on the project's background research. The second chapter includes a concise description of all facts relevant to the examination of the dual-wavelength passive Q-switched fiber pulsed laser generation by D-shape Fiber and MAX-Phase. Explanation of the dual-wavelength in literature review based on previously published Q-Switched, Fiber laser, saturable absorber (SA), D-shape and related 2D-material. The official journal, article, reference materials, and research papers are utilized to comprehend the concept and the design. The methods utilized to achieve the project's objectives are described in Chapter 3. Chapter 3 outlines the project's methodology, which consists of a set of interconnected practices, methods, and processes. This methodology guides the delivery of the research from beginning to end, ensuring its successful completion and closure. A brief review of the methodology employed for this chapter. In addition, this chapter divided into three parts under techniques of experimental work which are D-shape fiber fabrication, preparation of MAX-Phase (2D-material) and ring cavity of passive Q-Switched Fiber laser. In the meanwhile, Chapter 4 analyses the results and discussion, which covers the technical data of the dual-wavelength passive Q-switched pulsed fiber laser generated by using D-shaped, the optical components utilized in the project, and results in the form of tables and graphs. Besides that, end with the Chapter 5 that is the conclusion and future works that suggests more research to enhance the proposed method about this project.

Continued with last part of this thesis is about references, list of publications, papers presented, and also appendices where refer to journals, books, articles and research to complete this whole project.



CHAPTER 2

RESEARCH BACKGROUND



This chapter discussed and focused on the methods and equipment used by previous researchers that similar to this research. There are many researches with the same purpose and features as the project, but the arrangement of components, the material used, and the parameters differ. After thoroughly researched, suitable methods and materials will be selected and applied to this research to increase the efficiency of the project. The literature review has been summarized with related evidence which can answer the research objectives and research questions.

2.1 Overview of Fiber Laser

This section provides an overview of the fundamental principles of laser physics in these systems, as well as the waveguide designs that are used to enhance device performance. It also discusses the spectroscopy and nonlinear limitations that are associated with fibers. The text provides a comprehensive overview of the significant experimental findings from the past ten years. These findings cover various operating regimes of fiber lasers and encompass both commercially applicable fiber laser systems and the most recent advanced research utilizing innovative fiber designs. Fiber laser sources generate output with a high level of coherence and minimal noise, utilizing laser diodes for pumping.

Continuous wave (CW) lasers and pulsed lasers are two fundamental types of lasers, and these principles can be applied to fiber lasers as well. Continuous Wave (CW) emit a continuous and constant beam of light over time. The laser output remains at a steady state without any interruptions. CW lasers are characterized by a constant power output, providing a continuous stream of energy.

Besides, fiber pulsed lasers can achieve very high peak power levels during the short pulse duration, even if their average power is lower than that of CW lasers. The ability to deliver high peak powers in short pulses is crucial for certain processes. Pulsed lasers are more effective in certain material processing applications by minimizing heat transfer to the surrounding material, reducing the risk of thermal damage. Pulsed lasers can be designed with lower average power levels while still achieving high peak powers[1]. In summary, pulsed fiber lasers are often preferred in

applications that require precise material interaction, high peak powers, and reduced thermal effects.

2.2 Fiber pulsed laser

Recently, there has been significant research interest in the use of pulsed lasers for various applications, including medicine, telecommunications, and material processing [2], [3]. Compared to continuous-wave lasers, pulsed lasers have several advantages, such as increased pulse energy and peak power. There are two methods for generating a pulsed laser which are active and passive technique. The active technique necessitates the use of supplementary equipment, such as mirrors, lenses, and U-bench units. Nevertheless, the incorporation of those devices into the laser system resulted in additional insertion loss and increased complexity in the preparation procedure. Passive techniques are usually used to generate pulsed lasers by utilizing the saturable absorption mechanism of specific materials within the laser cavity. Saturable absorbers (SAs) are materials that have reduced absorption capacity as the intensity of light increases. They are usually used in laser cavities.

2.3 Passive Technique

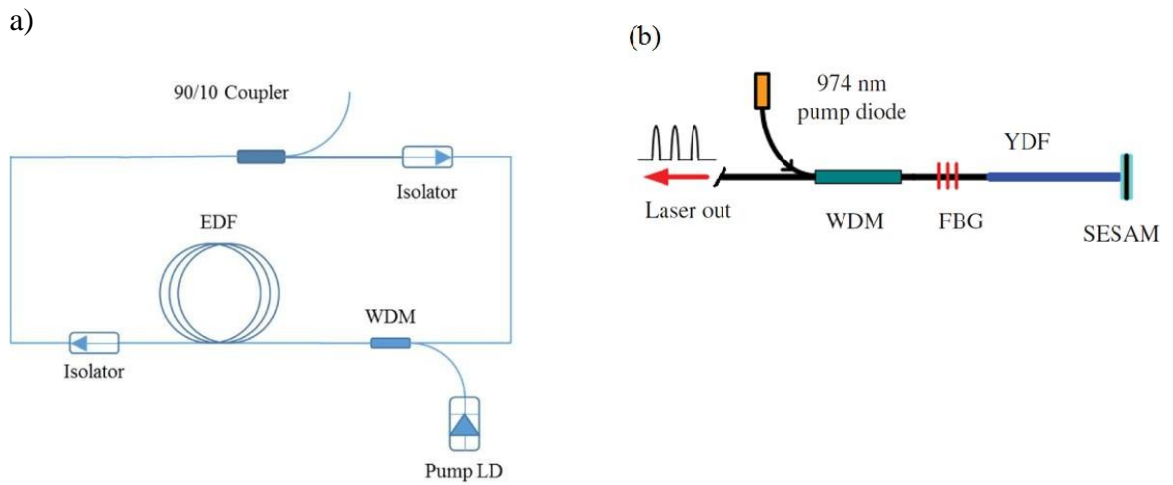


Figure 2.1: a) Ring Cavity b) Linear cavity

Fiber lasers have the benefits of being compact, dependable, cost-efficient, requiring no alignment, and requiring no maintenance. Fiber lasers, which offer the benefits of both fiber lasers, have been extensively studied and widely employed for diverse applications. *Figure 2.1b* illustrates that a typical fiber laser, with a linear cavity configuration and a long length of fiber, is unable to generate a laser output with a single frequency. This limitation is caused by spatial-hole burning in the gain medium. Typically, this issue is resolved by using a ring cavity. The laser cavity consists of a length of fiber that contains either bulk optic mirrors or fiber Bragg gratings that have been inscribed in the fiber core.

The fiber ring laser depicted in *Figure 2.1a* is highly appealing for laser development due to its ability to provide high gain and wide wavelength tunability. This is achieved by incorporating a wavelength tunable component into the ring cavity, utilizing the advantages of the long fiber cavity. As a result, this laser configuration offers both high output power and a broad range of tunable wavelengths. A ring-cavity design is more appropriate for a fiber laser due to the

absence of spatial hole-burning effect in a travelling-wave field. This design results in lower phase noise and a smaller linewidth compared to a linear cavity configuration. The gain fiber is stimulated by a pump laser source using a wavelength division multiplexer (WDM). The laser's unidirectional propagation within the fiber ring cavity is achieved through the use of an isolator, and the laser is extracted from the fiber ring via the help of a fiber coupler.

2.4 Ring Cavity

Fiber lasers utilize a doped silica glass fiber as the lasing medium and are triggered by diode lasers. Erbium-Doped Fiber (EDF), Ytterbium-Doped Fiber (YDF), and Thulium-Doped Fiber (TDF) are rare-earth-doped fibers employed as gain media in fiber lasers. The ring cavity of the Erbium-Doped Fiber Laser (EDFL) has the ability to amplify signals directly within the 1550 nm wavelength range, making it well-suited for applications such as optical amplifiers. The Ytterbium-doped fiber (YDF) ring cavity operates at a wavelength of approximately 1060 nm, while the Thulium-doped fiber (TDF) ring cavity operates at a wavelength of around 2 μm . In a passive ring cavity configuration, the laser cavity does not require external modulators to generate pulsed output. Instead, the generation of pulses can be achieved by utilizing the inherent properties of the gain medium and the design of the cavity. Erbium-doped fiber exhibits stable and sustained performance, making it highly suitable for passive ring cavity configurations.

2.5 Erbium Doped Fiber Laser (EDFL)

EDFLs have the capability to function across a variety of wavelength ranges, ranging from the visible spectrum to the far infrared spectrum. Erbium-doped fiber lasers (EDFL) emit laser at a wavelength of 1.5 μm and provide a broader range of frequencies, greater amplification, and reduced signal loss compared to alternative laser systems [4]. Initial efforts to create an EDFL involved utilizing argon-ion lasers as a means of generating the necessary energy. By 1995, the utilization of these lasers led to the development of commercial 1.55- μm fiber lasers. Pulse fiber lasers function by utilizing Q-switching and mode-locking techniques, which can be classified into active and passive method. The active method includes the utilization of an external modulator to accurately alter the losses in the resonator, in perfect synchronization with the laser cavity round-trips. The modulator is generally large in size and has a restricted ability to respond quickly in the generation of ultrashort pulses [5]. The passive method involves the integration of a suitable saturable absorber (SA) into the laser cavity.

Mode-locking is a laser process that creates ultrashort pulses of intense coherent light by synchronizing the longitudinal modes within the laser cavity [6].

Researchers have shown great interest in Q-switched lasers due to their ability to produce high pulse energy and adjustable pulse widths ranging from microseconds to hundreds of nanoseconds. McClung et al. reported the initial exhibition of Q-switched laser employing Ruby laser in 1962. Mears et al. introduced the Q-switched erbium-doped fiber laser (EDFL) after a period of twenty years. This was the initial instance of a pulsed laser utilizing a fiber that contained an active material. Q-

switched pulsed Erbium-Doped Fiber Lasers (EDFLs) generate pulsed laser output by actively or passively manipulating the loss within the laser cavity.

Q-switching is preferable over mode-locking because it has a simpler operation, improved stability, and higher pulse energies. This makes it suitable for applications that need reliable and strong high-energy pulses.

2.6 Q-Switched Pulse Laser

The generation of Q-switched pulses in active and passive modes is achieved by adjusting the Q-factor in the fiber laser cavity using the method [7], [8]. Active Q-switching requires a device that amplifies the losses within the cavity, functioning as a gate that periodically opens for a short time to decrease losses and enable the accumulation of a Q-switched pulse. The technique for producing ultrashort pulsed lasers are Q-switched operation at various wavelengths, which typically requires the use of an active or passive pulse modulator [21]. Active Q-switching typically requires an external signal, which is commonly regulated by an acoustic-optic or electro-optic modulator. The intracavity loss is periodically modified by an externally observed sinusoidal frequency.

2.7 Passive Q-Switched Pulse Laser

During the initial period, the majority of Q-switching lasers were produced through an active technique that involved the use of an externally controlled modulator, such as an acousto-optic or electro-optic device [9]. Nevertheless, this

technique presents various drawbacks, including its large size, difficulty in handling, and relatively high cost. Therefore, in order to address the issue, passive techniques have been extensively investigated. They possess various benefits in relation to manufacturing, structure, expenses, straightforwardness, effectiveness, and incorporation [10].

Within a cavity containing a SESAM, the SESAM acts as one of the mirrors of the cavity. The oscillating light is directed towards the dielectric reflector. SESAMs have several physical limitations, including their large size, lack of flexibility, limited working range, low resistance to damage, inability to function as input/output couplers, complex fabrication process [11], [12], high cost, narrow operational bandwidth [13], and the need for precise spatial alignment. These limitations make them impractical for use in fiber laser systems.

Passive techniques can be generated through using of an artificial or real saturable absorber (SA). Saturable absorbers (SAs) are commonly incorporated into the laser structure as unpumped sections of the laser cavity for the purpose of passive Q-switching. In this case, the high threshold that relates to it guarantees the accumulation of a substantial carrier density prior to the pulse. Additionally, the saturation of the SA during the pulse helps in increasing the peak power and reducing the duration. This regime combines characteristics of passive QS. Furthermore, the rapid recovery of the SA can prevent the occurrence of trailing pulses.

2.8 Saturable Absorber (SA)



Figure 2.2: Artificial and real saturable absorbers.

Saturation absorption refers to a condition where the optical loss decreases as the intensity of light increases. The transmission of light is determined by the change in light flux. Saturable absorbers (SAs) are optical devices that exploit a nonlinear phenomenon to convert continuous light into pulsed laser with high peak power and short pulse duration within fiber laser cavities [15], [16]. The SA is an essential material used for passive Q-switched. It can be classified into two types which are artificial and real, as depicted in *Figure 2.2*.

Artificial (SAs) involve the generation of a similar SA by exploiting nonlinear optical phenomena, such as the nonlinear polarization rotator and the nonlinear optical loop mirror [27, 28]. This review focuses on real SA rather than artificial SA. Artificial SAs are primarily represented by the nonlinear polarization rotation (NPR) [17], nonlinear amplifying loop-mirror (NALM) [18], and nonlinear optical loop mirror (NOLM) [19]. Artificial SAs are large in size and susceptible to environmental factors such as fiber movement, temperature, and vibration, resulting in reduced efficiency of reproduction.

2.9 Real Saturable Absorber



Figure 2.3: Classification of low-dimensional materials SA for fiber lasers.

On the other hand, real SA overcomes the drawback of artificial SA by offering a device that is more robust and stable in terms of mechanics and environment. This is achieved through the use of material structures in 0D, 1D and 2D material structures as shown in *Figure 2.3*. Recently, there has been significant growth in low-dimensional materials, including quantum dots, nanowires, graphene, and topological insulators. This has resulted to the rapid development of ultrafast fiber lasers that are based on low-dimensional materials and utilize vector solitons. This presents a comprehensive review of the latest developments in fiber lasers with low-dimensional materials saturable absorber, specifically focusing on vector soliton generation. The categorization of these materials is based on their dimensions, which include 0D, 1D, 2D, and other emerging materials [20]. 0D materials, such as quantum dots (QDs), present a quantum confinement effect and their saturable absorption is enhanced by the edge effect. Consequently, they are commonly employed as saturable absorbers (SAs) in optoelectronic devices. Furthermore, the properties of quantum dots (QDs) can be readily adjusted by altering their dimensions. Due to their unique structural arrangement and energy band distribution,

various 1D nanomaterials such as nanotubes, nanorods, and nanowires display significant nonlinear optical behavior at specific wavelengths. In 2009, researchers first investigated the use of 2D graphene as an optical saturable absorber (SA) in passive continuous-wave mode-locked lasers. Since then, an increasing number of other 2D materials, have been successively developed. This led to a swift advancement of novel self-assembled (SA) materials based on two-dimensional (2D) structures.

2.10 2D-Material

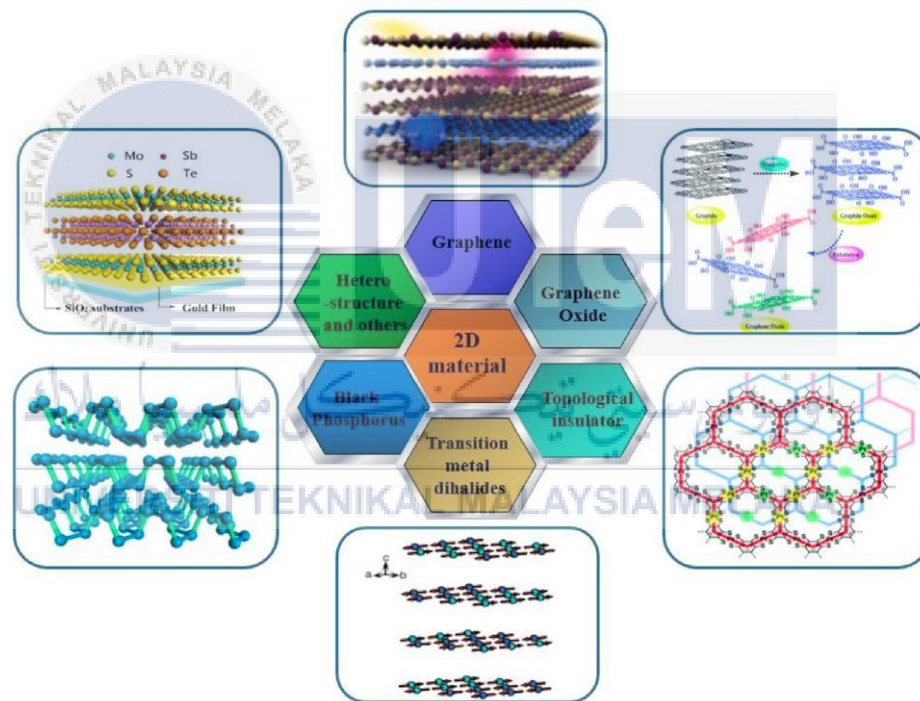


Figure 2.4: The 2D materials SA.

The use of 2D materials is common in the fabrication of saturable absorber (SA) devices due to their numerous advantages. These include the low insertion loss of the material. Additionally, the electronic properties of the material are easily controlled by adjusting factors such as doping, defects, and thickness.

Furthermore, 2D materials are easy to stack, allowing for the formation of multilayer structures and heterojunctions. The 2D materials depicted in *Figure 2.4*, such as graphene, topological insulators (TIs), black phosphorus (BP), and transition metal dichalcogenides (TMDs), have undergone extensive studied and published due to their unique properties compare to larger counterparts [21], [22].

Graphene is the initial 2D material that was discovered, and it was first suggested as SA in 2009. Ferrari et al. conducted a comprehensive analysis of the photonics and optoelectronics characteristics of graphene. Graphene exhibits a limited interaction with light and has a low modulation depth, which diminishes its non-linear effect [25].

Topological insulators (TIs) exhibit a wide nonlinear response due to their small absorption bandwidth and low damage thresholds [26].

BP is a 2D material that has basic cells with intrinsic anisotropy in the plane and a structure resembling a puckered honeycomb. It exhibits a strong interaction between light and matter and has a direct bandgap that can be adjusted across a wide range of wavelengths [27], [28], [29], [30]. However, BP shows the limitation in poor environmental stability towards oxidation sensitive within several hours to days, especially for monolayer and few-layer BP structures [31], [32], unstable in the ambient atmosphere, low damage threshold, and passable non-linear absorption [37].

The use of TMD exhibits various limitations. The wide energy gap of certain bulk (TMDs) in the visible and infrared regions restricts their use in optoelectronic

devices [33]. Another problem with the TMD is its low optical damage threshold under high power illumination. Transition metal dichalcogenide (TMD) based saturable absorbers (SAs) have a complicated fabrication process and lower damage thresholds compared to other SAs. This may restrict their application in high-power ultrafast lasers [34].

The MXenes exhibit electrical conductivity and hydrophilicity, making them highly promising as functional materials across various domains. Subsequently, the key concerns regarding MXene research encompass the procedure for preparation, microstructure, and MXene composites.

MAX-Phases are ternary carbides/nitrides with a layered structure, typically studied and produced as ceramic materials. By selectively eliminating a layer from MAX-Phases, it is possible to synthesize with MXenes, which possess a two-dimensional (2D) structure. The crack healing properties of MAX-Phase are highlighted among the different properties. MAX-Phases are a class of compounds consisting of layered carbides and nitrides. They have a general formula of $M_{n+1}AX_n$, where n ranges from 1 to 4. In this formula, M represents an early transition metal, A represents a group A element, and X can be either carbon, nitrogen, or both. Some examples of common MAX-Phases include Ti_3SiC_2 , Ti_3AlC_2 , Ti_2AlC , V_2AlC , Ti_2AlN . Presently, there exist more than 90 MAX-Phases. The experimentally created MAX-Phases may consist of various constitutive elements. Furthermore, there are ongoing theoretical predictions of additional constitutive elements of MAX-Phases, as well as continued synthesis of more MAX-Phases.

In 2019, MAX-Phases SAs found to serve as alternatives to MXenes SAs by Lee et al. [63]. The metal-ceramic MAX-Phases SAs are the promising solution to the challenge faced by MXenes SAs, yet, possess similar advantages to them with reasonable price [64]. The most vital contribution of the MAX-Phases SAs is their simple fabrication techniques without involving any hazardous substances.

2.11 MAX-Phase as $(\text{Ti}_3\text{Al}(\text{C}_{0.5}, \text{N}_{0.5})_2)$

The MAX-Phases possess unique physical properties such as exceptional resistance to oxidation, a high modulus of elasticity, low density, and a high melting temperature. These properties make it a valuable material for various industrial applications [35]. Compared to other 2D materials, it was easily employed as a SA without the need for a laborious preparation process. The laser cavity successfully generates a pulsed laser at a modulation depth of 2-60% in the 1.55- μm wavelength range. This is achieved using erbium-, ytterbium-, and thulium-doped fiber laser cavity [36], [37]. MAX-Phases possess a combination of ceramic and metallic properties. MAX-Phases have similar properties to metals, such as thermal and electrical conductivity, machinability with conventional tools, and resistance to thermal shock. Additionally, they exhibit ceramic-like characteristics including high strength, excellent high temperature strength, and thermal stability.

2.12 Integration of SA

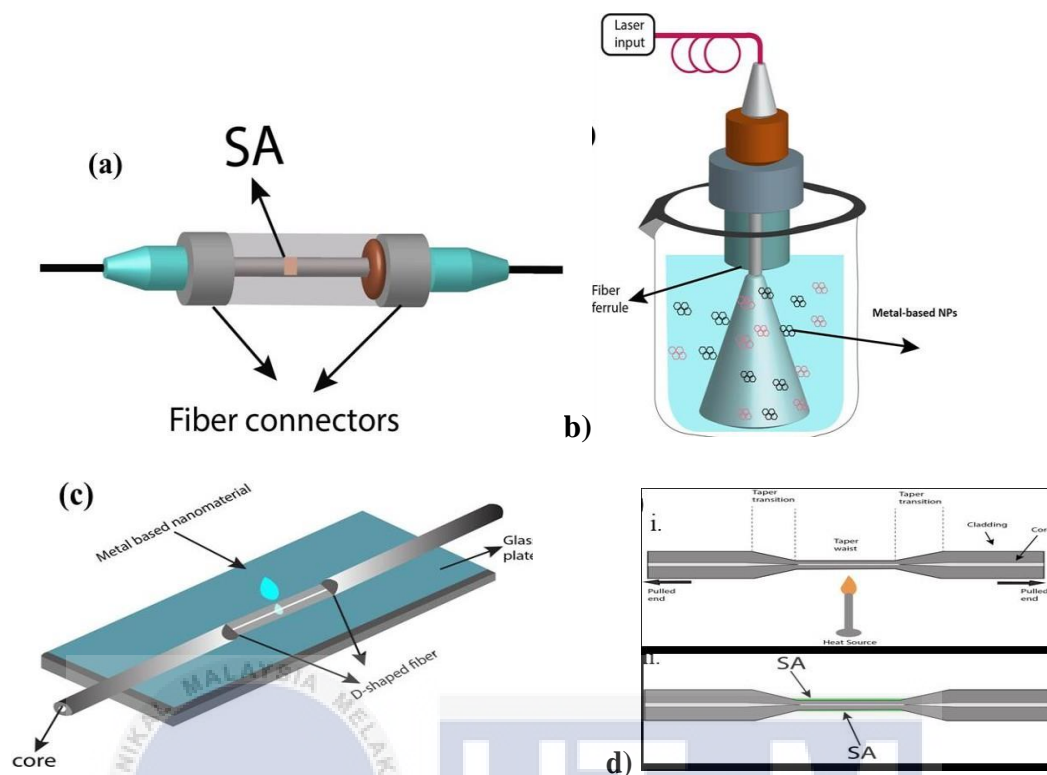


Figure 2.5: Integration Methods of SA. (a) Thin film-based SA is positioned between two fibers connectors. (b) Optical deposition technique. (c) Optical fiber with a D-shaped cross-section having metal-based nanomaterial deposited on the waist. (d) Tapered optical fiber. i) tapering process ii) deposited SA on microfiber waist.

The performance of lasers can be significantly enhanced by using suitable SA structures. Typically, thin films (*Figure 2.5a*) are produced at low cost and ambient temperature. For SA structures, both pure nanomaterial films and hybrid films have been effectively used. The produced polymer solutions and metallic nanoparticles are thoroughly combined by using stirring or ultrasonication in the polymer film technique before being deposited onto the substrate to dry.

The production of tapered optical fiber is commonly accomplished by applying heat to a small portion of the fiber while simultaneously stretching both ends of the

fiber, as depicted in *Figure 2.5d*. Potential heat sources for tapering fibers include a gas burner flame [38], high-power laser pulses [39], or chemical etching [40]. The process of flame tapering involves the application of a gas burner flame to a specific region of fiber. By carefully heating the fiber in the flame, it becomes softened to create a tapered region.

2.13 D-Shape Fiber Optic

Instead of using a fiber ferrule SA, the microfiber fully exploits the nonlinear absorption properties of the material by interacting with the evanescent field. The D-shaped fibers are formed by selectively removing the cladding in the radial direction of the regular fiber, exposing the core, as illustrated in *Figure 2.5c*. SAs (*Figure 2.5b*) are commonly deposited on the polished side of the fiber using techniques like optical deposition, magnetic sputtering deposition, and others [41]. The interaction takes place via the use of the SA coating in combination with the evanescent field produced by the light propagating from the polished surface of the D-shaped fiber. Therefore, the strength of the evanescent field can be controlled by altering the depth of polishing [42]. Furthermore, when compared to fiber ferrule SA, D-shaped fiber produces a higher power output as a result of the decreased intensity of the evanescent field with SA [43]. The durability of this fiber surpasses that of tapered fiber. Nevertheless, the D-shaped SA shows polarization-dependent loss, which is determined by transverse magnetic and transverse electric polarizations. The loss causes instability in the performance of SA, demanding precise control of the polarization state. In 2019, Niu et al. employed the ion beam sputter technique to apply GNPs onto a D-shaped optical fiber. In 2021, Muhammad et al. utilized an

electron beam deposition technique to incorporate single nucleotide polymorphisms (SNPs) onto an optical fiber with a D-shaped cross-section [44]. By using a D-shaped fiber as a saturable absorber (SA), the fiber laser cavity achieves a longer interaction length, resulting in a higher quality optical nonlinearity. Furthermore, it enhanced the optical damage threshold of the SA device and reduced the instability of the pulsed laser under high pumping power. In addition, the use of D-shaped fiber might reduce the occurrence of photo-darkening caused by the polymer matrix and the burning effect on the tip of the fiber-ferrule.



CHAPTER 3

METHODOLOGY



Figure 3.0 shows the methodology for the development of the Q-switched fiber laser with a saturable absorber based on a MAX-Phase (2D material) and integrated with a D-shaped fiber optic, involves a multi-step process. Firstly, a suitable 2D material, acting as a saturable absorber, is carefully chosen and integrated into the fiber laser system. This material is crucial for achieving Q-switching, allowing for the generation of short and high-energy pulses. The Q-switched mechanism is then implemented within the fiber laser cavity, enhancing control over pulse characteristics. Simultaneously, a D-shaped fiber optic, tailored for efficient mode coupling and wavelength division, is incorporated to facilitate dual-wavelength operation. The geometric parameters of the D-shaped fiber are optimized to ensure effective interaction with the saturable absorber and promote

stable Q-switched. This comprehensive integration of Q-switching, saturable absorber technology, and the D-shaped fiber optic is aimed at achieving a compact, efficient, and versatile dual-wavelength fiber pulsed laser.

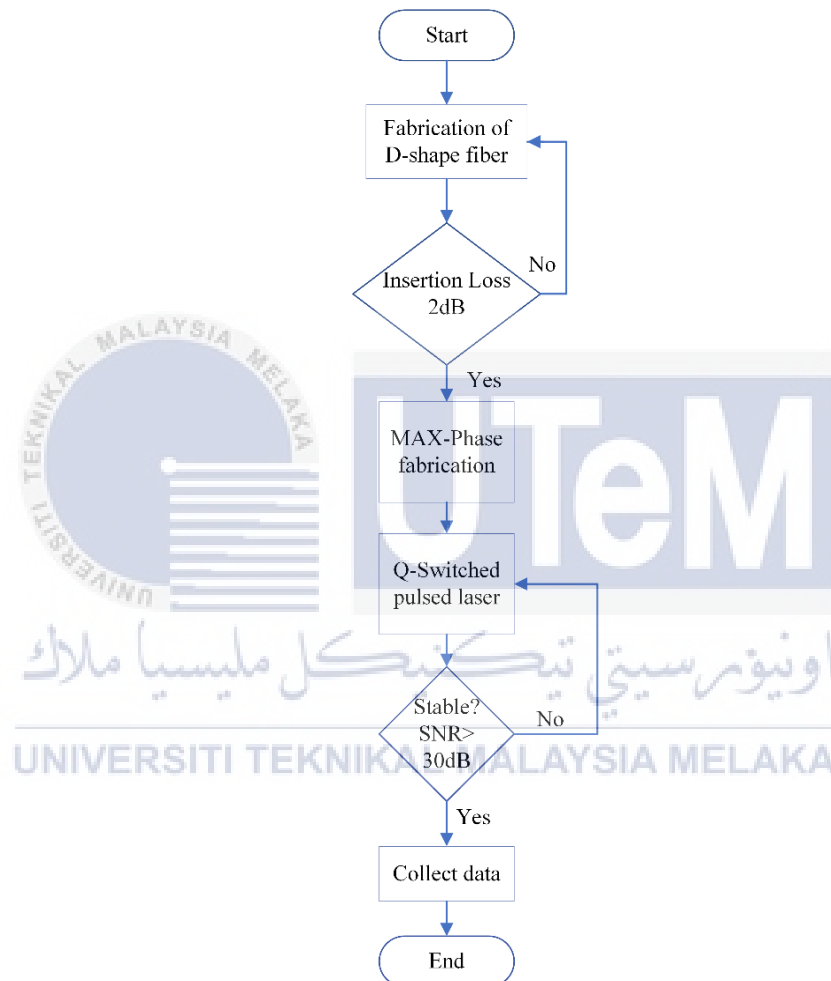


Figure 3.0: Flow chart of methodology.

3.2 Methods and passive technique used for experimental work

The experimental work attempts to generate a dual-wavelength passive Q-switched fiber laser by utilizing $(\text{Ti}_3\text{Al}(\text{Co}_{0.5}, \text{Ni}_{0.5})_2)$ MAX-Phase as a saturable absorber on a D-shaped fiber. The research involves a carefully designed sequence of

methods and techniques to achieve accurate manipulation of the laser output. The methods and technique used for this experimental work have separated into 3 major parts which are fabrication of D-shape fiber optic, preparation of $(\text{Ti}_3\text{Al}(\text{C}_{0.5}, \text{N}_{0.5})_2)$ MAX-Phase and configuration for ring cavity of passive Q-switched.

3.2.1 Fabrication of D-shape Fiber Optic

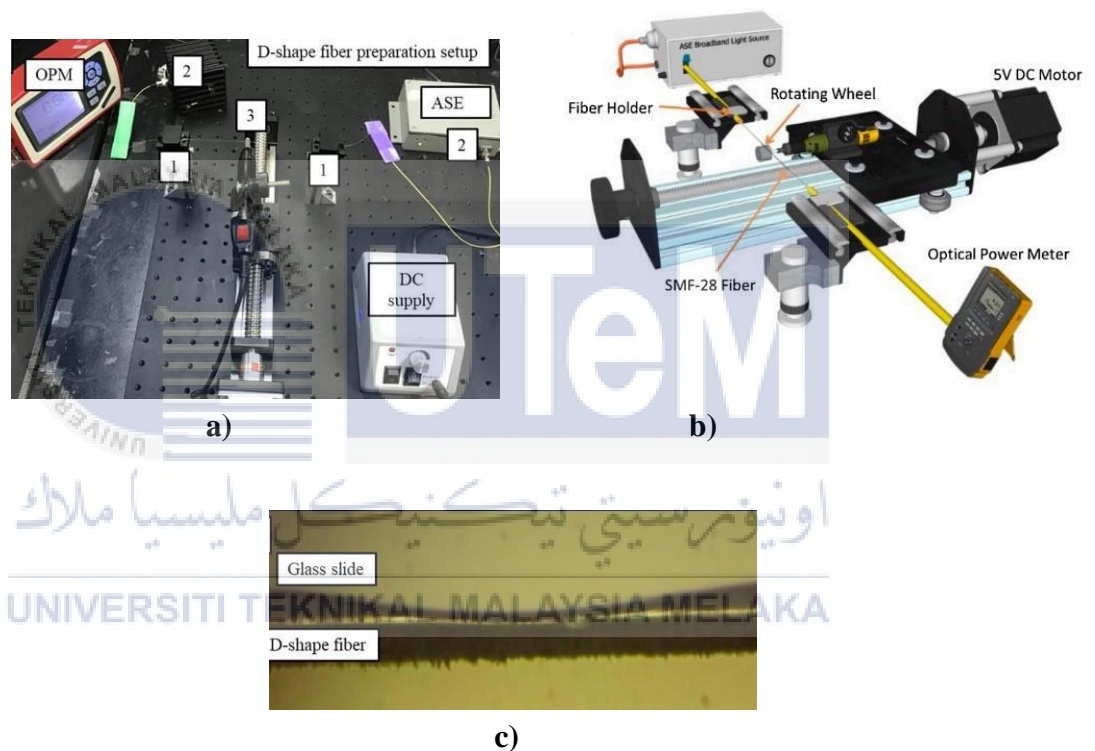


Figure 3.1: a) D-shape fiber preparation setup. b) Graphical demonstration for mechanical D-shape fiber fabrication. c) Microscopic image of the D-shape fiber.

The designed D-shaped fiber polisher, as depicted in **Figure 3.1**. The proposed experimental setup consists of an amplified stimulated emission (ASE) broadband light source, a mechanical wheel with sandpaper, a 5-volt (5 V) DC motor, an optical power meter, an adjustable stage, and a pair of fiber holders.

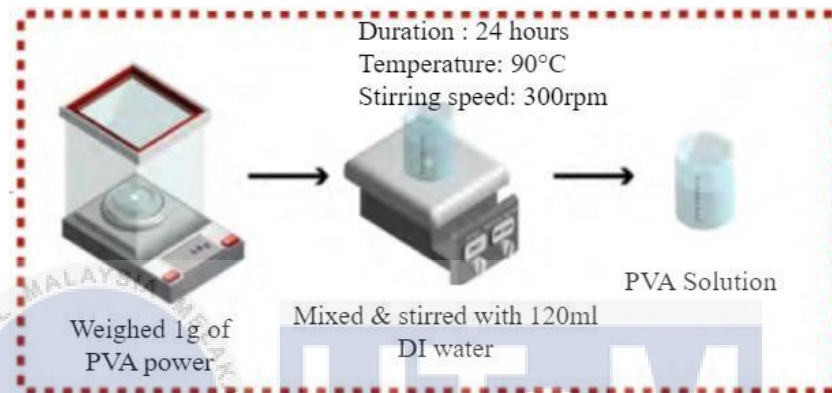
The experimental procedure starts by splicing two fiber-ferrules with a single-mode optical fiber (SMF-28). Approximately 5 mm of fiber coat was removed to expose the cladding of SMF-28. The SMF-28 was deployed with two fiber holders as a clamper and connected to the ASE source, the other end launched onto an optical power meter. The 5 V DC motor was turn on after properly adjusted the mechanical wheel with sandpaper so that it touches the uncoated region of SMF-28. The real-time measurement ensures an appropriate amount of cladding was removed.



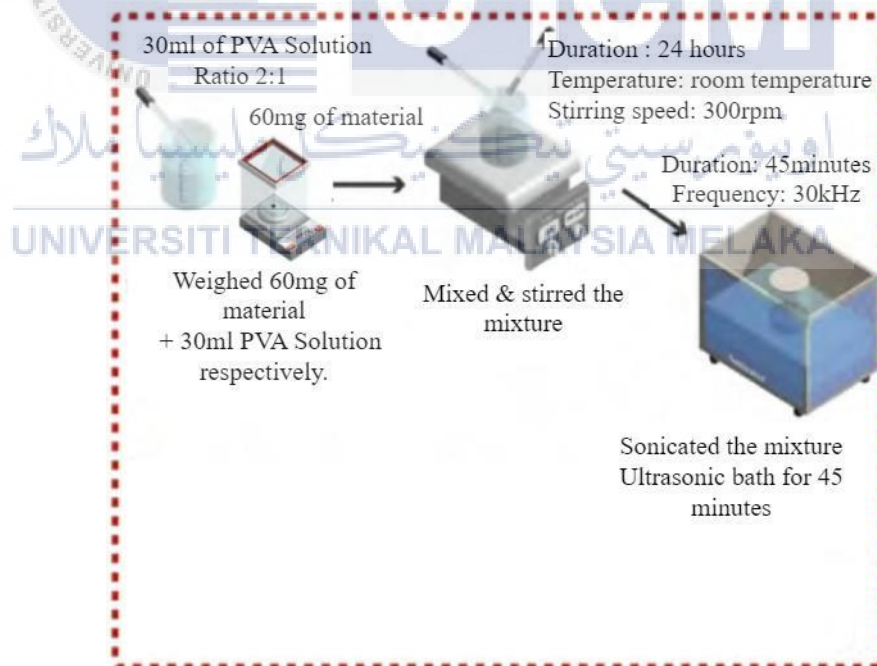
3.2.2 Preparation of $(\text{Ti}_3\text{Al}(\text{C}_{0.5}\text{N}_{0.5})_2)$ MAX-Phase



a)



b)



c)

Figure 3.2: a) $\text{Ti}_3\text{Al}(\text{C}_{0.5}\text{N}_{0.5})_2$ MAX-Phase solution. b) Preparation of PVA Solution. c) Fabrication of $(\text{Ti}_3\text{Al}(\text{C}_{0.5}\text{N}_{0.5})_2)$ MAX-Phase.

The D-shaped fiber fabrication process was completed in just 15 minutes, guaranteeing a rapid preparation procedure for surface area (SA) analysis. The process of synthesizing the $(\text{Ti}_3\text{Al}(\text{C}_{0.5}, \text{N}_{0.5})_2)$ powder and PVA solution involves the use of liquid-phase exfoliation (LPE) technique. The liquid-phase exfoliation (LPE) technique used a colorless, odorless, easily manageable, environmentally-friendly, and cost-effective PVA as the host polymer to achieve atomic adhesion of the $(\text{Ti}_3\text{Al}(\text{C}_{0.5}, \text{N}_{0.5})_2)$. The mentioned technique is relatively straightforward, practical and cost-effective, as it requires no precise control and innovative fabrication tools.

At first, in **Figure 3.2b**, the process began by measuring 1 g of PVA powder using an electronic balance. The powder was then mixed with 120 ml of deionized (DI) water using a hot plate stirrer. This mixture was stirred continuously at a temperature of 90°C and a stirring speed of 300 rpm for a duration of 24 hours until complete dissolution was achieved. The usage of PVA as a host material offers several benefits, such as being non-toxic, cost-effective, possessing excellent mechanical and thermal properties, and exhibiting enhanced interfacial adhesion with reinforcing materials such as fibers. The mixture was stirred on a heated surface for a duration of 24 hours at ambient temperature, with a stirring rate of 300 rpm. The 60 mg $(\text{Ti}_3\text{Al}(\text{C}_{0.5}, \text{N}_{0.5})_2)$ powder was added to a beaker containing 30 ml of PVA solution with a ratio of 2:1, as depicted in **Figure 3.2c**. Afterwards, the powder underwent complete dissolution through stirring via a magnetic stirrer for a duration of 24 hours at room temperature, with a stirring speed of 300 rpm. The thoroughly mixed solution was subsequently subjected to sonication for a duration of 45

minutes, employing an ultrasonic bath operating at an average frequency of 30 kHz. This process aimed to agitate the particles of the material ($\text{Ti}_3\text{Al}(\text{Co}_{0.5}, \text{Ni}_{0.5})_2$) in order to achieve a uniform distribution. This step was repeated three times. Next, the remaining MAX-Phase solution was transferred into a tube and effectively employed as a SA for D-shaped fiber. This resulted in obtained a functional of a functional MAX-Phase solution, as depicted in *Figure 3.2a*.

The MAX-DS was directly spliced into the EDFL. The MAX-Phase solution was applied onto the polished side of the D-shaped fiber structure SA using a micropipette until a consistent pulse train was observed on the oscilloscope.



3.2.3 Configuration for Ring Cavity of Passive Q-Switched

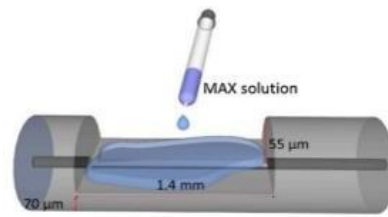


Figure 3.3: MAX-Phase solution for integration.

For the Q-switching pulse technique, the $(\text{Ti}_3\text{Al}(\text{C}_{0.5}, \text{N}_{0.5})_2)$ MAX-Phase in **Figure 3.3** act as saturable absorber properties played a major role. Pulsed laser technique characterization was employed to understand and optimize the saturable absorption behavior of the material. The laser cavity was carefully adjusted to exploit the saturable absorption characteristics of the $(\text{Ti}_3\text{Al}(\text{C}_{0.5}, \text{N}_{0.5})_2)$ D-shaped fiber that lead to the passive Q-switched of the fiber laser.

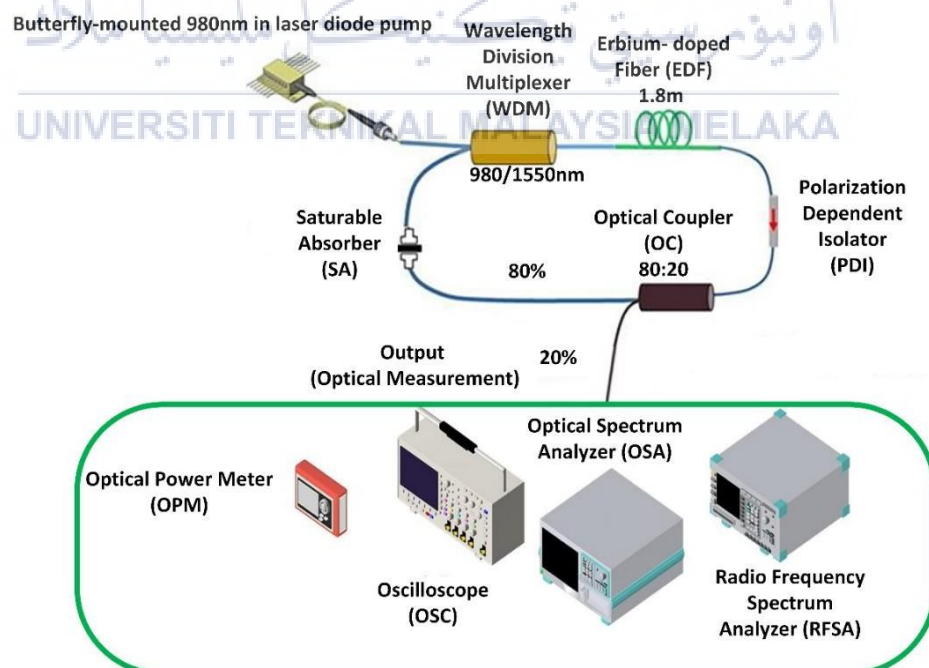


Figure 3.4: The schematic arrangement of $(\text{Ti}_3\text{Al}(\text{C}_{0.5}, \text{N}_{0.5})_2)$ D-shape fiber based the Q-switched EDFL.

Figure 3.4 shows the configuration of the proposed Q-switched EDFL based on a ring cavity scheme with the in-placed $(\text{Ti}_3\text{Al}(\text{Co}_{0.5}\text{N}_{0.5})_2)$ D-shape fiber SA. In this experiment, the $(\text{Ti}_3\text{Al}(\text{Co}_{0.5}\text{N}_{0.5})_2)$ as MAX-Phase is applied on D-shape which incorporated inside EDFL by a pair of fiber connector because the D-shape fiber cable has two peak tail. Prior to applying the MAX-Phase on the D-shape fiber, the ferrule surface was cleaned using alcohol. Subsequently, a visual inspection microscope was used to check for dirt on the ferrule in order to minimize high in connector loss, high reflectance, and the contamination of transceivers [56]. The EDFL cavity comprises a 1.8 m long Erbium-Doped Fiber (EDF) as the gain medium, a 980 nm laser diode connected through a 980/1550 wavelength division multiplexer (WDM), an optical isolator, an 80:20 optical coupler, and SAs. The gain medium consists of a 1.8 m long erbium-doped fiber (EDF) that is optically stimulated by a butterfly-mounted 980 nm laser diode pump. This stimulation produces a pulsed laser using a wavelength division multiplexer (WDM) with a wavelength of 980/1550 nm. The EDF has a central diameter measuring 4 μm , a numerical aperture of 0.24, and a core absorption rate of 24 dB/m at a wavelength of 1550 nm. The polarization dependent isolator (PDI) enables the laser to pass through in a single direction while blocking light in the opposite direction. The 80:20 optical coupler splits the optical power, allowing 80% of the portion to pass through the ring cavity for additional amplification, while directing 20% of the output to various optical measurements. The MAX-Phase D-shape fiber SA modulates its absorption properties according to the intensity of the laser entering the ring cavity. It functions as a passive Q-switched, allowing the laser to generate short laser pulses.

The digital oscilloscope with an integrated RF spectrum analyzer is used to measure the temporal characteristics of the generated pulses, such as the pulse train

and RF spectrum. On the other hand, the optical spectrum analyzer is used to observe the spectral and intensity-dependent characteristics of the Q-switched EDFL. The measurements are facilitated by a 1.2 GHz photodetector (PD, InGaAs) with high gain and low noise characteristics. This photodetector converts the optical signal into the corresponding electrical signal. An optical power meter is used to monitor the output power of the pulsed laser. The overall length of the cavity for MAX-DS was 14.6m.



CHAPTER 4



In this chapter, the result analysis of the research as well as the passive Q-switched Fiber Laser of the ring cavity is discussed to evaluate system performance across wavelength of C-band region and characterize pulse dynamics. Data collection and results of experimental work are recorded and discussed in this chapter. For information, this research is to mainly produce a dual-wavelength fiber pulsed laser. MAX-Phase as $(\text{Ti}_3\text{Al} (\text{C}_{0.5}, \text{N}_{0.5})_2)$ is aided to generate the dual-wavelength of passive Q-switched pulse laser by applying MAX-Phase on D-shaped fiber as saturable absorber.

Table 1.0: Tabulation of raw data of the experimental work.

EXPERIMENT: Q-switched D-Shaped Fiber ($Ti_3Al(C_{0.5}, N_{0.5})_2$)									
Day:		Tuesday				Location:		Photonic Lab (UM)	
Date:		19/09/2023				Name:		Ronald Raj	
Time:		10:00 - 19:00				Code:		20230919	
No.	Laser Input		Oscilloscope			OPM	Pulse Energy (nJ)	Peak Power (mW)	
	Input (mA)	Input (mW)	Frequency (kHz)	Pulse Width (μs)	Pulse Period (μs)	Output Power (mW)			
1	140	38.058	35.34	6.58	28.3	1.5	42.44482	6.45058	
2	150	42.218	37.45	5.84	26.7	1.8	48.06409	8.23015	
3	160	46.378	39.53	5.3	25.3	2.1	53.12421	10.02344	
4	170	50.538	41.22	4.94	24.26	2.4	58.22416	11.78627	
5	180	54.698	42.55	4.62	23.5	2.7	63.45476	13.7348	
6	190	58.858	44.26	4.32	22.59	3.1	70.04067	16.21312	
7	200	63.018	45.83	4.12	21.82	3.4	74.18721	18.00661	
8	210	67.178	48.19	3.89	20.75	3.7	76.77941	19.73764	
9	220	71.338	49.55	3.72	20.18	4.1	82.7447	22.2432	
10	230	75.498	51.92	3.57	19.26	4.4	84.74576	23.73831	

Table 1.0 shows the parameters of the dual-wavelength laser output involves spectral analysis, measurement of out power performances, and the temporal behaviour of the fiber pulses. Throughout the experimental work, the temporal laser output is monitoring using oscilloscope to characterize the pulse width, pulse period and repetition rate. The dual-wavelength is observed by choose peak output power and its wavelength using optical spectrum analyzer (OSA). Then, pump power is adjusted to find the optimal conditions for passive Q-switching. Real-time monitoring and adjustments were made on optical power meter (OPM) to optimize the laser performance and ensure the stable operation of the dual-wavelength Q-switched fiber laser.

4.1 Q-switched Laser Performance

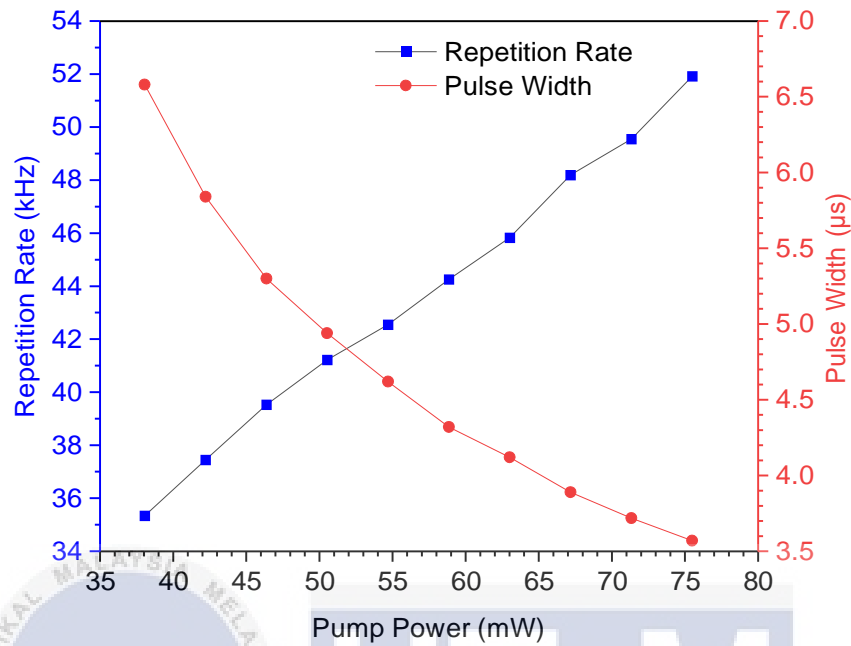


Figure 4.0: The relation of the repetition rate and pulse width against ascending pump power.

The Q-switched laser is being investigated with the $(\text{Ti}_3\text{Al}(\text{Co}_{0.5}\text{N}_{0.5})_2)$ saturable absorber device incorporated into the ring cavity. The Q-switched laser initiated with an initial repetition rate of 35.34 kHz once the pump power reached the threshold pump power of 38.06 mW. The Q-switched laser-maintained stability as the pump power was gradually increased to 75.5 mW. **Figure 4.0** shows that the repetition rate increases in a nearly straight line from 35.34 to 51.92 kHz as the pump power increases from 38.06 to 75.5 mW. However, the pulse width decreases from 6.58 to 3.57 μs as the laser cavity experiences gain compression and the pump power increases. Moreover, higher pump power contributes to a faster SA saturation, because of the population inversion which repeats in a faster manner.

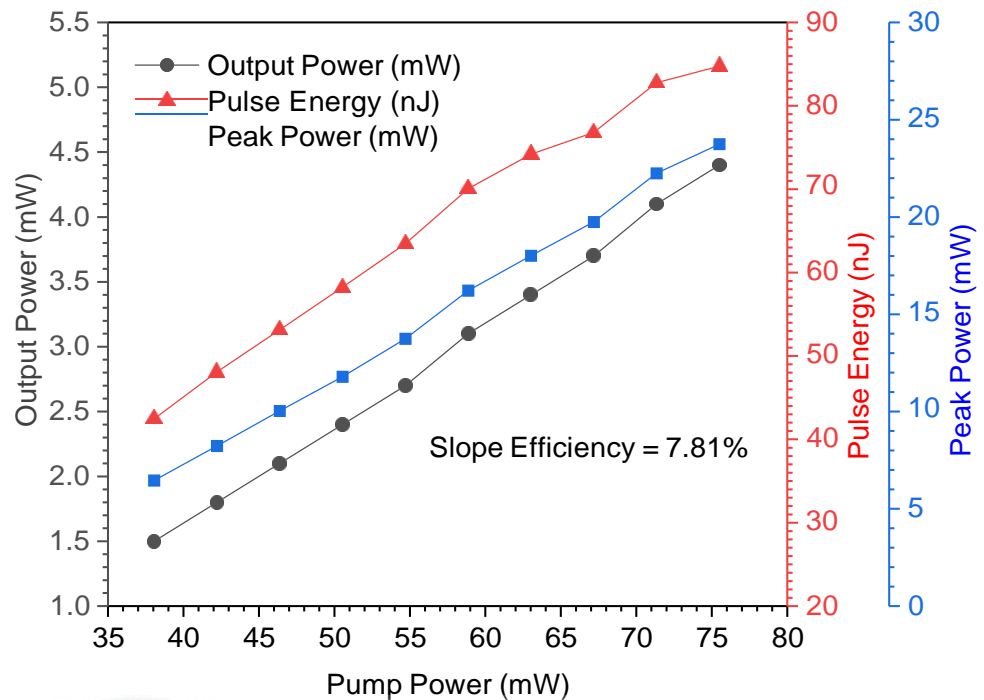


Figure 4.1: The output power, pulse energy, and peak power of the Q-switched EDFL at different pump power settings.

Figure 4.1 illustrates the changes in average output power, peak power, and pulse energy across a range of pump power levels, which range from 38.06 to 75.5 mW. The output power indicates a linear increase, ranging from 1.5 to 4.4 mW. The slope efficiency, which measures the rate of change, is calculated to be 7.81%. The slope efficiency, defined as the output power (mW), is determined using the formula $y=mx+c$. The calculated peak power increases almost linearly, ranging from 6.45 to 23.74 mW. In addition, the pulse energy increases from 42.44 nJ to 84.74 nJ. **Equation 1** and **Equation 2** represent the mathematical expressions for pulse energy and peak power, respectively.

$$\text{Pulse Energy (nJ)} = \frac{\text{Output power (mW)}}{\text{Repetition Rate (kHz)}} \quad (\text{Equation 1})$$

$$\text{Peak power (mW)} = \frac{\text{Pulse Energy (nJ)}}{\text{Pulse width (\mu s)}} \quad (\text{Equation 2})$$



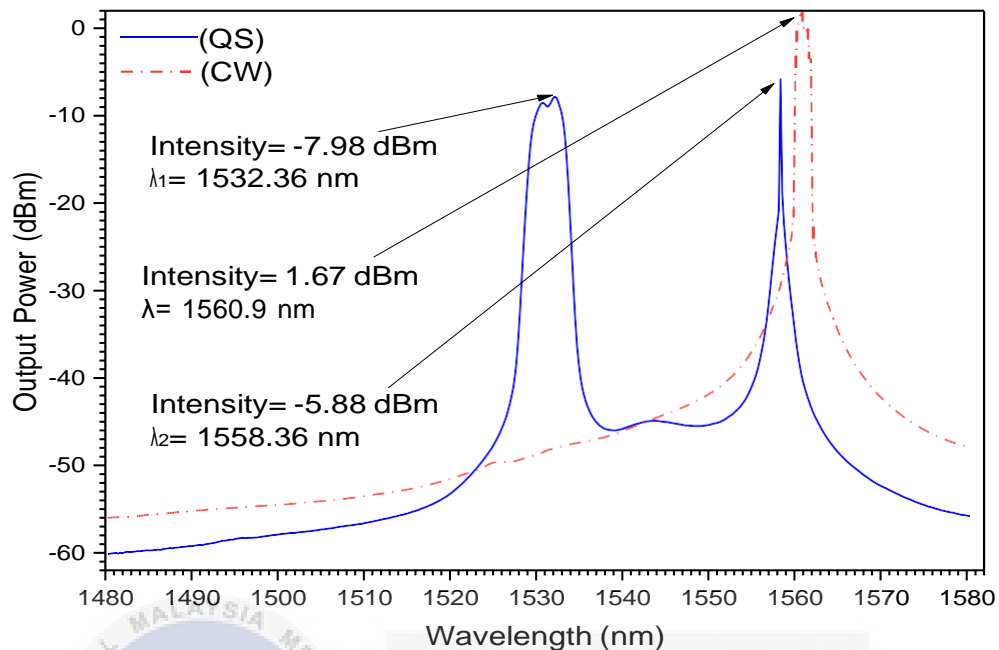
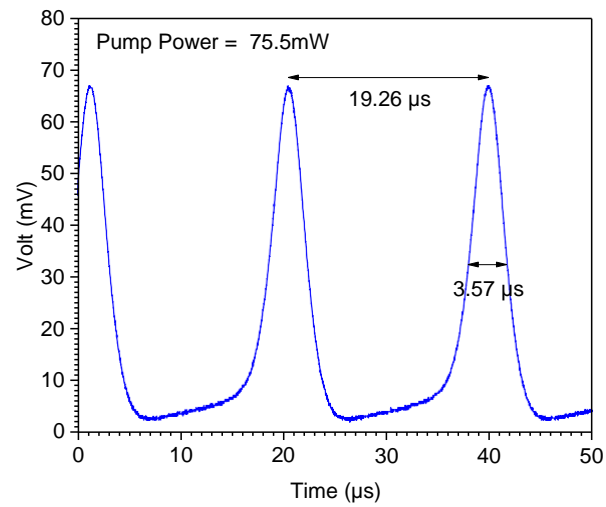


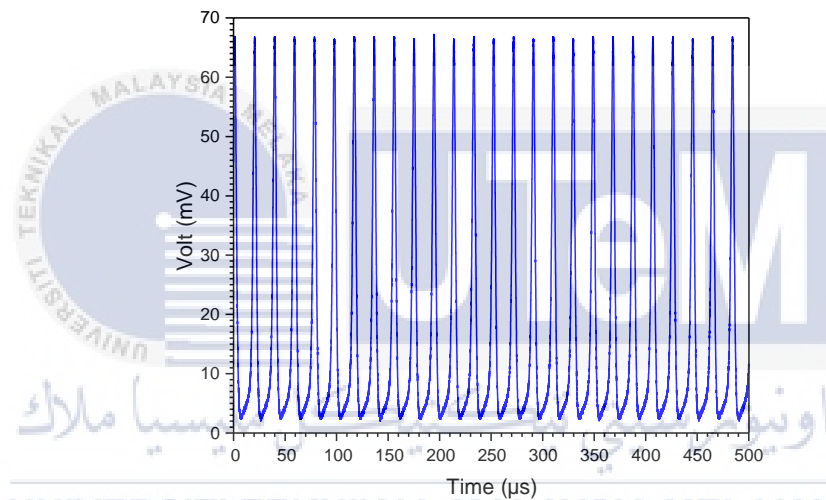
Figure 4.2: The output spectrum of the Q-switched laser and CW laser at the 75.5 mW pump power.

The optical spectrum of the output Q-switched laser at a pump power of 75.5 mW is depicted in **Figure 4.2**. This graph represents the dual-wavelength of a passive Q-switched laser. A D-shaped fiber is integrated into the EDFL cavity along with a pair of fiber-ferrules. The laser spectrum remains continuous without the presence of a saturable absorber (SA). The continuous wave (CW) laser achieved a greater peak intensity of 1.67 dBm and a longer central wavelength, λ , measuring 1560.9 nm. The incorporation of a bare D-shaped fiber results in a leftward shift of the Q-switched dual-wavelength due to the insertion of a saturable absorber (SA) in the cavity. However, no pulses are observed on the oscilloscope even when the pump power is adjusted within the range of 38.06 - 75.5 mW. Five drops of the prepared MAX-Phase solution were applied onto the D-shaped fiber to initiate the pulses. Following a duration of 15 minutes, the liquid began evaporation, resulting in the

appearance of visible Q-switching pulses on the oscilloscope. The D-shaped fiber, which contains a MAX-Phase solution, adjusts the loss within the laser cavity by exploiting the interaction between the evanescent field of the light (photon) and the SA (electron). This interaction leads to the generation of Q-switched pulses. The measurement of the temporal pulse trace involves capturing the frozen signal at the highest achievable pump power during stable Q-switching, which was 75.5 mW. During the procedure, the laser diode is activated and the pump power is adjusted to 75.5 mW. On the other hand, the OSA's spectrum peak shifted to indicate the successful generation of pulsed laser. A narrower red-shifted gap reflects a lower occurrence of losses. The first peak intensity of the Q-switched spectrum is -7.98 dBm and is located at a wavelength of $\lambda_1=1532.36$ nm, while the second peak intensity of the Q-switched spectrum is -5.88 dBm and is located at a wavelength of $\lambda_2=1558.36$ nm. The peak output power of the Q-switched spectrum shrinks compared to the continuous wave (CW) spectrum because of the splitting of power between the dual Q-switched spectrum. The Q-switched spectrum has been demonstrated to display dual-wavelength lies within the C-band region, specifically between 1530 and 1565 nm. The SA acts as a loss modulator, leading to population inversion.



a)



b)

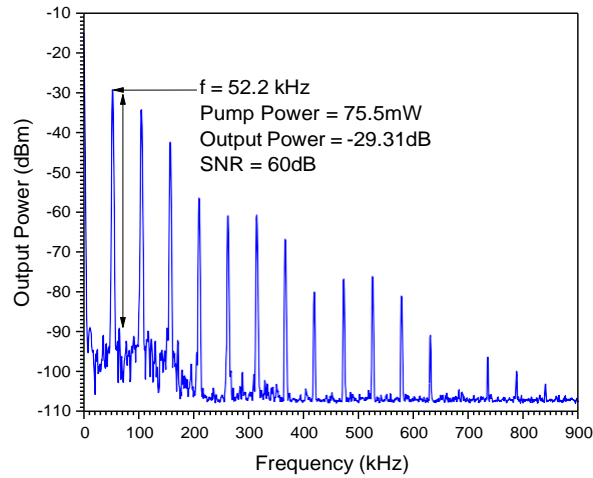
Figure 4.3: *a) The two-envelope pulse train. b) oscilloscope trace (the pulses within a longer time frame).*

Figure 4.3a displays the pulse train of the two envelopes as a function of time, which was recorded at the maximum achievable pump power of 75.5mW. The pulse peak separation, also known as the pulse period, is measured to be 19.26 μs , which is proportional to a pulse frequency of 51.92 kHz. The pulse's full width at half maximum (FWHM) which is also equivalent to the pulse width is given as 3.57 μs .

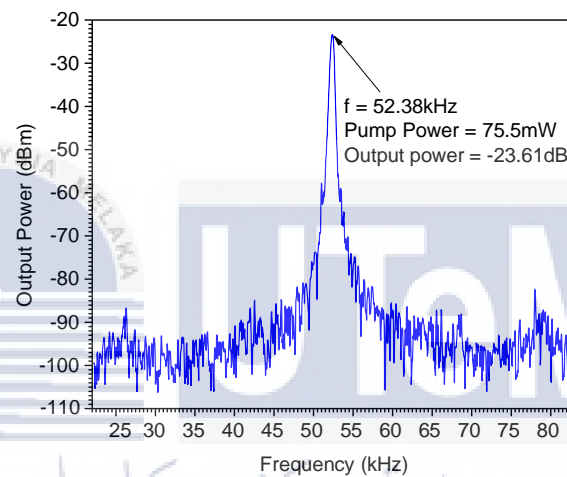
Figure 4.3b demonstrates a pulse train consisting of multiple pulses occurring within

a 500 μ s interval. The pulse train provides steady peak intensity, indicating a high level of stability with minimal jittering.





a)



b)

Figure 4.4: a) The RF spectrum of the pulsed laser with span of 900kHz.

b) The enlargement of the fundamental frequency spectrum.

The RF spectrum, which represents the frequency domain, is used to validate the fundamental frequency. This analysis is conducted at a pump power of 75.5 mW, as shown in **Figure 4.4a**. The fundamental frequency is 52.38 kHz, as shown in **Figure 4.4b**, and is very similar to the RF harmonics at 52.2 kHz. It has quite a significant signal-to-noise ratio (SNR) of 60 dB. The oscilloscope analysis of the RF harmonics in the time domain indicates that there is no significant spectrum damage, which further suggests the stability of the produced Q-switched laser.

4.2 Comparisons of previous research

Table 2.0: Laser output performance comparison of Q-switched EDFL by using various SA materials.

SAs	Method	Q-Switching Threshold (mW)	Min. Pulse Width (μ s)	Max. Repetition Rate (kHz)	Max. Output Power (mW)	Max. Pulse Energy (nJ)	SNR (dB)	Ref.
rGO	DSF	32.43	2.01	54.1	0.405	7.499	55	[45]
MoS ₂	DSF	14.8	3.19	25.27	2.27	90	-	[46]
WS ₂	DSF	186	0.71	134	2.5	19	-	[47]
Bi ₂ Te ₃	DSF	17.3	2.81	42.8	0.55	12.7	-	[38]
Ti ₃ C ₂ T _x	DSF	81	2.58	77.52	10.4	134.2	63	[48]
Ti ₂ AlC	OD	30	4.88	27.45	0.62	22.58	-	[49]
Ti ₂ AlC	TF	88	0.99	46.3	4.75	102.7	60	[50]
Ti ₃ AlC ₂	TF	44	3.93	112	8.4	75	66	[51]
Ti ₃ AlC ₂	DSF	62	2.93	96.15	14.6	151.8	70	[37]
(Ti ₃ Al (C _{0.5} , N _{0.5}) ₂)	TF	24.9	6.6	46.3	0.49	10.54	49	[52]
(Ti ₃ Al (C _{0.5} , N _{0.5}) ₂)	DSF	38.06	3.57	51.92	4.4	84.75	60	This work

The performance of the Q-switched laser generated by (Ti₃Al (C_{0.5}, N_{0.5})₂) in the EDFL cavity shows several improvements in laser parameters compared to another SA based on MAX-Phase, as shown in **Table 2.0**. The pulsed laser emitted by the SA devices that were created were also compared to the other 2D materials that were applied onto D-shaped fiber. The materials used in this study include reduced graphene oxide (rGO), molybdenum disulfide (MoS₂), tungsten disulfide (WS₂), bismuth telluride (Bi₂Te₃), and titanium carbide (Ti₃C₂T_x). The MAX-DS achieved the maximum repetition rate compared to other self-assembled MAX-Phase structures. Nevertheless, the D-shaped fibre coated with WS₂ demonstrates a higher

repetition rate of 134 kHz [47]. According to the table, the $(\text{Ti}_3\text{Al}(\text{C}_{0.5}\text{N}_{0.5})_2)$ (DSF) has a greater pulse energy compared to the Ti_3AlC_2 (TF) [51] and Ti_2AlC (OD) [49]. Additionally, it has a significantly lower threshold pump power compared to most of the other MAX-Phase SAs being compared. Therefore, the Q-switched pulse laser has the capability to generate at a lower pump power. MAX-DS improved the highest achievable output power, pulse energy, and signal-to-noise ratio of the generated Q-switched laser, surpassing previous studies using MAX-Phase or other 2D materials. The improvement in the quality of saturable absorption (SA), including non-saturable loss and saturable absorption, enabled the achievement of Q-switched at a low pump power, as demonstrated in previous studies [46, 38]. The pulse width is improved by optimizing the length of the gain medium and the arrangement of optical components in the EDFL.



CHAPTER 5



The results or outcomes of this project are explained by conclusion and future works. Future recommendations are based on the results of the report, after conclusions. This chapter describes two parts. The first section addresses the findings and highlights the findings that support the main objectives of the research in the previous chapter. The second part includes a recommendation on how to improve the experimental work in future.

5.1 Conclusion

To conclude, this research effectively satisfied the primary objectives of developing a dual-wavelength passive Q-switched fiber pulsed laser using a MAX-Phase and D-shaped fiber setup, and validating the $(\text{Ti}_3\text{Al}(\text{C}_{0.5}\text{N}_{0.5})_2)$ MAX-Phase and D-shaped fiber as a saturable absorber. The EDFL fiber laser setup effectively generated a dual-wavelength passive Q-switched fiber pulsed laser spectrum at $\lambda_1=1532.36$ nm and $\lambda_2=1558.36$ nm by including the $(\text{Ti}_3\text{Al}(\text{C}_{0.5}\text{N}_{0.5})_2)$ MAX-DS SA. The experimental results proved that the MAX-Phase and D-shaped fiber exhibit saturable absorber properties, enabling effective Q-switching operation in the C-band region. The MAX-Phase SA is integrated into the EDFL ring cavity by incorporating it onto a D-shaped fiber. The Q-switched laser shows a consistent presence when the pump power reaches a threshold of 38.06 mW and can maintain operating up to 75.5 mW. At a pump power of 75.5 mW, the system achieves a maximum operating repetition rate of 51.92 kHz and the shortest pulse width of 3.57 μs . MAX-DS achieved Q-switched operation with an output power of 4.4 mW, a peak power of 23.74 mW, and a pulse energy of 84.75 nJ. These values were obtained at a pump power of 75.5 mW, which is the highest achievable level. Furthermore, the laser output exhibits a consistent pulse shape and intensity, with a signal-to-noise ratio (SNR) of 60 dB and an optical-to-optical efficiency of 7.81%. The findings demonstrated that the fiber laser exhibits a high pulse energy (nJ) and the lowest required pump power (mW) in compared with previous research. Therefore, it becomes easier to generate a stable Q-switched dual-wavelength of MAX-DS as a saturable absorber in the erbium-doped fiber laser (EDFL) ring cavity. The experimental results show that the MAX-Phase material, specifically

($\text{Ti}_3\text{Al}(\text{Co}_{0.5}\text{Ni}_{0.5})_2$), has the potential to function as a saturable absorber. The demonstration highlights the use of a D-shaped fiber to amplify pulses in a Q-switched Erbium-Doped Fiber Laser (EDFL).

5.2 Future works

In light of the successful realization of a dual-wavelength passive Q-switched fiber laser using MAX-Phase ($\text{Ti}_3\text{Al}(\text{Co}_{0.5}\text{Ni}_{0.5})_2$) and D-shaped fiber as a saturable absorber, several avenues for future research and recommendations emerge. Firstly, the optimization of the laser system parameters, such as pump power, cavity length, and saturable absorber characteristics, could be explored to further enhance the performance of the dual-wavelength laser. The results are demonstrated by completing in generate Q-switched pulsing technique, so it can be used for mode-locking pulsing technique too. Then, it also has high chance to generate multi-wavelength by some modification on SA structure such as dual-notch D-shape, S-M-S and D S-M-S (integrated with MZI- Mach Zehnder Interferometer). Passive Q-switched fiber lasers operating at multiple wavelengths, which offer the benefits of being compact, having multiple channels for oscillation, and exhibiting Q-switching characteristics, have garnered significant interest due to their potential applications in high-precision fiber sensing and lidar systems [1]. The lasers consist of a Q-switched element and a multi-channel component. To ensure design flexibility and functionality, it is desirable for multi-wavelength Q-switched fiber lasers to possess adjustable wavelength-number and wavelength-separation [53].

Furthermore, the investigation into the stability and long-term reliability of the

laser system is essential for practical applications. Understanding the impact of environmental factors on the dual-wavelength laser's performance and implementing measures to mitigate these effects will be crucial. C-band region has generated Q-switched pulsed laser, believe that apply same material and method while using different ring cavity and gain medium to produce fiber pulsed laser on L and S band region.

Furthermore, the EDFL has received extensive research attention since its initial research publication by Mears et al. in 1981. The widespread use of EDFL in fiber-optic telecommunication is due to its excellent compatibility with fiber-optic telecommunication, low crosstalk, and high output power. However, it is also worth investigating its potential applications in other mid-infrared regions.

Collaboration with researchers could also contribute to the development of MAX-Phase materials with tailored properties for enhanced saturable absorption. Exploring different types of saturable absorbers and their integration with D-shaped fibers could provide insights into alternative configurations for advanced laser functionalities. This may involve fine-tuning the D-shaped fiber structure and exploring different compositions of MAX-Phase materials for improved saturable absorption. New nanomaterials, such as 2D, provides reliable choices for SAs. However, the LPE technique is a simple and efficient method for fabricate 2D nanomaterials from bulk crystals on a large scale, while maintaining high stability under normal environmental conditions [54]. The sonication process can effectively minimize sample contamination using a non-contact sonicate [54]. Conversely, nanomaterials are more susceptible to damage from high pump power as a result of

the photothermal effect of Metal [55]. Therefore, it is expected that by employing stabilization techniques or alternative methods, the damage threshold will be further improved in future investigations.

In terms of recommendations, disseminating the findings through peer-reviewed publications and presentations at conferences would contribute to the broader scientific community's understanding of the capabilities and potential applications of the developed dual-wavelength laser system. Collaborative efforts with industry partners could facilitate the transition of this technology from the laboratory to practical applications, fostering innovation in various fields. The Q-switched technique excels in producing high-energy pulses, making it suitable for specific applications in different domains.

In summarized, the future work and recommendations center around the refinement of the dual-wavelength passive Q-switched fiber laser system, its optimization for specific applications, and the exploration of materials and configurations. These efforts will not only contribute to the advancement of laser technology but also expand the practical applications of such systems in diverse industries.

REFERENCES

- [1] S. A. Sadeq, S. K. Al-Hayali, S. W. Harun, and A. Al-Janabi, "Copper oxide nanomaterial saturable absorber as a new passive Q-switcher in erbium-doped fiber laser ring cavity configuration," *Results Phys*, vol. 10, pp. 264–269, Sep. 2018, doi: 10.1016/j.rinp.2018.06.006.
- [2] "Laser Treatment of Dark Skin _ American Journal of Clinical Dermatology".
- [3] S. Juodkazis, V. Mizeikis, and H. Misawa, "Three-dimensional microfabrication of materials by femtosecond lasers for photonics applications," *Journal of Applied Physics*, vol. 106, no. 5. 2009. doi: 10.1063/1.3216462.
- [4] D. Korobko *et al.*, "Stabilization of a harmonic mode-locking by shifting the carrier frequency," *Journal of Lightwave Technology*, vol. 39, no. 9, pp. 2980–2987, May 2021, doi: 10.1109/JLT.2021.3068822.
- [5] Koo, J. Lee, J. Jhon, and Y. M. Lee, "Femtosecond harmonic mode-locking of a fiber laser at 3.27 GHz using a bulk-like, MoSe₂-based saturable absorber," 2016.
- [6] J. Kim and Y. Song, "Ultralow-noise mode-locked fiber lasers and frequency combs: principles, status, and applications," *Adv Opt Photonics*, vol. 8, no. 3, p. 465, Sep. 2016, doi: 10.1364/aop.8.000465.
- [7] S. V. Garnov *et al.*, "Passive mode-locking with carbon nanotube saturable absorber in Nd: GdVO₄ and Nd:Y_{0.9}Gd_{0.1} VO₄ lasers operating at 1.3 μ m," *Laser Phys Lett*, vol. 4, no. 9, pp. 648–651, Sep. 2007, doi: 10.1002/lapl.200710040.
- [8] "You've Come a Long Way, Baby_ Persistent Gender Inequality in University

- Enrolment and Completion in Canada, 1979–2004 _ Canadian Public Policy”.
- [9] N. Mohd Yusoff *et al.*, “Low threshold Q-switched fiber laser incorporating titanium dioxide saturable absorber from waste material,” *Optik (Stuttg)*, vol. 218, Sep. 2020, doi: 10.1016/j.ijleo.2020.164998.
- [10] D. Dutta *et al.*, “Newly developed chromium-doped fiber as a saturable absorber at 1.55- and 2.0- μm regions for Q-switching pulses generation,” *Optical Fiber Technology*, vol. 48, pp. 144–150, Mar. 2019, doi: 10.1016/j.yofte.2019.01.010.
- [11] A. Zhang *et al.*, “Recent progress of two-dimensional materials for ultrafast photonics,” *Nanomaterials*, vol. 11, no. 7. MDPI AG, Jul. 01, 2021. doi: 10.3390/nano11071778.
- [12] H. Wu *et al.*, “Stable passively Q-switched erbium-doped fiber laser based on CuCrO₂ nanoparticles saturable absorber,” *Opt Commun*, vol. 475, Nov. 2020, doi: 10.1016/j.optcom.2020.126222.
- [13] “Stable 5-GHz fundamental repetition rate passively SESAM mode-locked Er-doped silica fiber lasers”.
- [14] J. W. You, S. R. Bongu, Q. Bao, and N. C. Panoiu, “Nonlinear optical properties and applications of 2D materials: Theoretical and experimental aspects,” *Nanophotonics*, vol. 8, no. 1. De Gruyter, pp. 63–97, 2018. doi: 10.1515/nanoph-2018-0106.
- [15] “Nanosized indium selenide saturable absorber for multiple solitons operation in Er³⁺-doped fiber laser”.
- [16] “Chromium oxide film for Q-switched and mode-locked pulse generation”.
- [17] V. J. Matsas, W. H. Loh, and D. J. Richardson, “Self-Starting, Passively Mode-Locked Fabry-Perot Fiber Soliton Laser Using Nonlinear Polarization

- Evolution,” *IEEE Photonics Technology Letters*, vol. 5, no. 5, pp. 492–494, 1993, doi: 10.1109/68.215258.
- [18] “Nonlinear amplifying loop mirror”.
- [19] “Nonlinear-optical loop mirror”.
- [20] Y. Qi *et al.*, “Recent advance of emerging low-dimensional materials for vector soliton generation in fiber lasers,” *Materials Today Physics*, vol. 23. Elsevier Ltd, Mar. 01, 2022. doi: 10.1016/j.mtphys.2022.100622.
- [21] “Graphene-dendritic polymer hybrids_ synthesis, properties, and applications _ Journal of the Iranian Chemical Society”.
- [22] M. Chhowalla, Z. Liu, and H. Zhang, “Two-dimensional transition metal dichalcogenide (TMD) nanosheets,” *Chemical Society Reviews*, vol. 44, no. 9. Royal Society of Chemistry, pp. 2584–2586, May 07, 2015. doi: 10.1039/c5cs90037a.
- [23] “Scopus - Print Document”.
- [24] Q. Bao *et al.*, “Atomic-layer graphene as a saturable absorber for ultrafast pulsed lasers,” *Adv Funct Mater*, vol. 19, no. 19, pp. 3077–3083, Oct. 2009, doi: 10.1002/adfm.200901007.
- [25] X. Zhu *et al.*, “Enhanced light-matter interactions in graphene-covered gold nanovoid arrays,” *Nano Lett*, vol. 13, no. 10, pp. 4690–4696, Oct. 2013, doi: 10.1021/nl402120t.
- [26] S. Chen *et al.*, “Few-Layer Topological Insulator for All-Optical Signal Processing Using the Nonlinear Kerr Effect,” *Adv Opt Mater*, vol. 3, no. 12, pp. 1769–1778, Dec. 2015, doi: 10.1002/adom.201500347.
- [27] S. Liu *et al.*, “Graphene/phosphorene nano-heterojunction: facile synthesis, nonlinear optics, and ultrafast photonics applications with enhanced

- performance,” *Photonics Res*, vol. 5, no. 6, p. 662, Dec. 2017, doi: 10.1364/prj.5.000662.
- [28] M. Zhang *et al.*, “2D Black Phosphorus Saturable Absorbers for Ultrafast Photonics,” *Advanced Optical Materials*, vol. 7, no. 1. Wiley-VCH Verlag, Jan. 04, 2019. doi: 10.1002/adom.201800224.
- [29] M. Zhang *et al.*, “2D Black Phosphorus Saturable Absorbers for Ultrafast Photonics,” *Advanced Optical Materials*, vol. 7, no. 1. Wiley-VCH Verlag, Jan. 04, 2019. doi: 10.1002/adom.201800224.
- [30] H. Jiang, H. Shi, X. Sun, and B. Gao, “Optical Anisotropy of Few-Layer Black Phosphorus Visualized by Scanning Polarization Modulation Microscopy,” *ACS Photonics*, vol. 5, no. 6, pp. 2509–2515, Jun. 2018, doi: 10.1021/acsp Photonics.8b00341.
- [31] “Antimonene_ a long-term stable two-dimensional saturable absorption material under ambient conditions for the mid-infrared spectral region”.
- [32] J. O. Island, G. A. Steele, H. S. J. Van Der Zant, and A. Castellanos-Gomez, “Environmental instability of few-layer black phosphorus,” *2d Mater*, vol. 2, no. 1, Jan. 2015, doi: 10.1088/2053-1583/2/1/011002.
- [33] Y. Xu *et al.*, “Solvothermal Synthesis and Ultrafast Photonics of Black Phosphorus Quantum Dots,” *Adv Opt Mater*, vol. 4, no. 8, pp. 1223–1229, Aug. 2016, doi: 10.1002/adom.201600214.
- [34] “Transition-metal dichalcogenides heterostructure saturable absorbers for ultrafast photonics”.
- [35] M. Dahlqvist, B. Alling, and J. Rosén, “Stability trends of MAX phases from first principles,” *Phys Rev B Condens Matter Mater Phys*, vol. 81, no. 22, Jun. 2010, doi: 10.1103/PhysRevB.81.220102.

- [36] “Ti₂AlC-based saturable absorber for passive Q-switching of a fiber laser”.
- [37] “Q-Switched YDFL generation by a MAX phase saturable absorber”.
- [38] R. Jarzebinska, C. S. Cheung, S. W. James, and R. P. Tatam, “Response of the transmission spectrum of tapered optical fibres to the deposition of a nanostructured coating,” *Meas Sci Technol*, vol. 20, no. 3, 2009, doi: 10.1088/0957-0233/20/3/034001.
- [39] Y. Zhang, A. Dhawan, and T. Vo-Dinh, “Design and fabrication of fiber-optic nanoprobe for optical sensing,” *Nanoscale Res Lett*, vol. 7, pp. 6–18, 2012, doi: 10.1007/s11671-010-9744-5.
- [40] “Parameter control, characterization, and optimization in the fabrication of optical fiber near-field probes”.
- [41] K. Y. Lau and D. Hou, “Recent research and advances of material-based saturable absorber in mode-locked fiber laser,” *Optics and Laser Technology*, vol. 137. Elsevier Ltd, May 01, 2021. doi: 10.1016/j.optlastec.2020.106826.
- [42] “Carbon nanotube mode lockers with enhanced nonlinearity via evanescent field interaction in D-shaped fibers”.
- [43] L. Li *et al.*, “Femtosecond passively Er-doped mode-locked fiber laser with WS₂ solution saturable absorber,” *IEEE Journal of Selected Topics in Quantum Electronics*, vol. 23, no. 1, pp. 44–49, Jan. 2017, doi: 10.1109/JSTQE.2016.2538640.
- [44] A. R. Muhammad *et al.*, “Evanescent field interaction of 1550 nm pulsed laser with silver nanomaterial coated D-shape fiber,” *Infrared Phys Technol*, vol. 119, Dec. 2021, doi: 10.1016/j.infrared.2021.103920.
- [45] H. Ahmad, M. Tajdidzadeh, and S. A. Reduan, “Passively Q-switched erbium-doped fiber laser using coated reduced graphene oxide on arc-shaped single

- mode optical fiber as a saturable absorber,” *Laser Phys*, vol. 28, no. 8, Aug. 2018, doi: 10.1088/1555-6611/aac1af.
- [46] H. Ahmad, H. Hassan, R. Safaei, K. Thambiratnam, M. F. Ismail, and I. S. Amiri, “Molybdenum disulfide side-polished fiber saturable absorber Q-switched fiber laser,” *Opt Commun*, vol. 400, pp. 55–60, Oct. 2017, doi: 10.1016/j.optcom.2017.04.071.
- [47] H. Ahmad, H. Hassan, R. Safaei, K. Thambiratnam, M. F. Ismail, and I. S. Amiri, “Molybdenum disulfide side-polished fiber saturable absorber Q-switched fiber laser,” *Opt Commun*, vol. 400, pp. 55–60, Oct. 2017, doi: 10.1016/j.optcom.2017.04.071.
- [48] A. A. A. Jafry *et al.*, “MXene Ti₃C₂T_x as a passive Q-switcher for erbium-doped fiber laser,” *Optical Fiber Technology*, vol. 58, Sep. 2020, doi: 10.1016/j.yofte.2020.102289.
- [49] “Ti₂AlC-based saturable absorber for passive Q-switching of a fiber laser”.
- [50] H. Ahmad, H. S. M. Albaqawi, N. Yusoff, W. Y. Chong, and M. Yasin, “Q-Switched Fiber Laser at 1.5 μ m Region Using Ti₃AlC₂ MAX Phase-Based Saturable Absorber,” *IEEE J Quantum Electron*, vol. 56, no. 2, Apr. 2020, doi: 10.1109/JQE.2019.2949798.
- [51] A. A. A. Jafry *et al.*, “MAX phase Ti₃AlC₂ embedded in PVA and deposited onto D-shaped fiber as a passive Q-switcher for erbium-doped fiber laser,” *Optik (Stuttg)*, vol. 224, Dec. 2020, doi: 10.1016/j.ijleo.2020.165682.
- [52] S. A. Anuar, M. F. A. Rahman, A. M. Nasir, A. A. Latiff, and A. A. A. Jafry, “Q-Switched Erbium-Doped Fiber Laser Generation using Titanium Aluminum Carbonitride Ti₃Al(C_{0.5}N_{0.5})₂ Saturable Absorber,” *Journal of Advanced Research in Applied Sciences and Engineering Technology*, vol. 31,

- no. 1, pp. 144–155, Jun. 2023, doi: 10.37934/araset.31.1.144155.
- [53] A. Zhang, C. Sun, H. Pan, X. Shi, W. Li, and Q. Cheng, “Characterization of multi-wavelength Q-switched fiber laser by changing wavelength separation of filter,” *Optical Fiber Technology*, vol. 58, Sep. 2020, doi: 10.1016/j.yofte.2020.102297.
- [54] J. Yin *et al.*, “Hafnium Sulfide Nanosheets for Ultrafast Photonic Device,” *Adv Opt Mater*, vol. 7, no. 5, Mar. 2019, doi: 10.1002/adom.201801303.
- [55] X. Chen, Y. Chen, M. Yan, and M. Qiu, “Nanosecond photothermal effects in plasmonic nanostructures,” *ACS Nano*, vol. 6, no. 3, pp. 2550–2557, Mar. 2012, doi: 10.1021/nn2050032.
- [56] “The FOA Reference For Fiber Optics - Inspection And Cleaning Of Fiber Optic Connectors,” www.thefoa.org.
<https://www.thefoa.org/tech/ref/testing/test/scope.html>
- [57] L. Arissian and J.-C. Diels, “Mode-Locked Lasers,” 2018.
<https://www.sciencedirect.com/topics/materials-science/fiber-laser>
- [58] “Saturable Absorber - an overview | ScienceDirect Topics,” www.sciencedirect.com.
<https://www.sciencedirect.com/topics/engineering/saturable-absorber> (accessed Jan. 13, 2024).

LIST OF PUBLICATIONS AND PAPERS PRESENTED

Published works as well as papers presented at conferences, seminars, symposiums etc pertaining to the research topic of the research report/ dissertation/ thesis are suggested be included in this section. The first page of the article may also be appended as reference.



APPENDICES

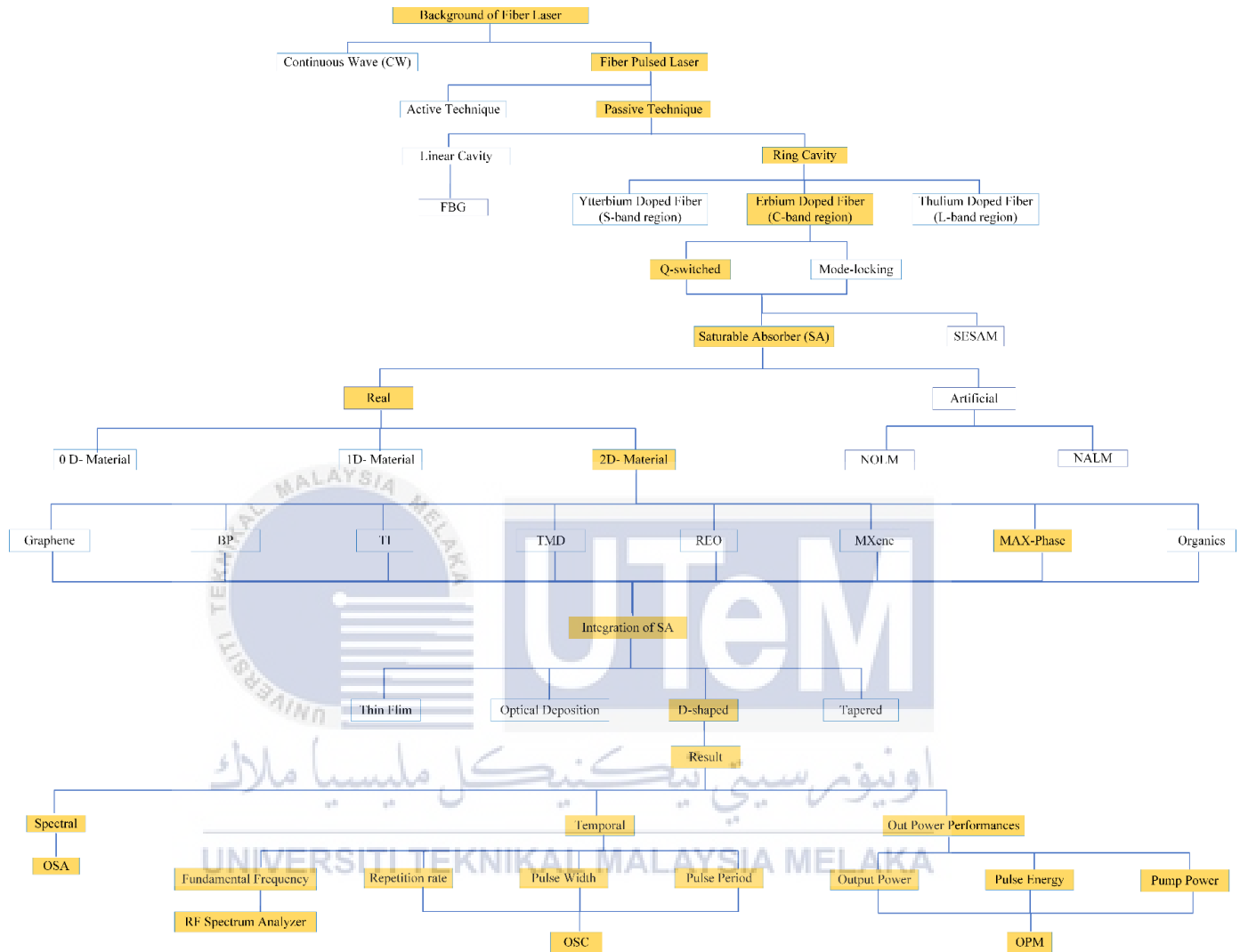


Figure 2.0: The literature studies are briefly demonstrated in form of K-chart.

The study conducted an experiment on a dual-wavelength passive Q-switched fiber laser by utilizing $(\text{Ti}_3\text{Al}(\text{Co}_{0.5}\text{Ni}_{0.5})_2)$ D-shaped fiber as a saturable absorber. The K-chart provides a visual representation of the method and material used as shown in **Figure 2.0**. The K-chart includes parameters under spectral, temporal and out power measurements. It assists in determining the best operating conditions, highlighting the impact of significant variables on the laser's efficiency, and

providing guidance for future adjustments to enhance better performance. The K-chart is a helpful tool for researchers and effectively evaluating the laser performance under different operational conditions. It provides a comprehensive understanding of the laser's capabilities for generating dual-wavelength Q-switched fiber laser.

